

Improving the ISBA_{CC} land surface model simulation of water and carbon fluxes and stocks over the Amazon forest

*E. Joetzjer¹, C. Delire¹, H. Douville¹, P. Ciais², B. Decharme¹, D. Carrer¹,
H. Verbeeck³, M. De Weirdt³, D. Bonal⁴*

¹CNRM-GAME UMR3589, Groupe d'étude de l'atmosphère météorologique, 31000 Toulouse, France

²Laboratory of Climate Sciences and the Environment (LSCE), Joint Unit of CEA-CNRS, L'Orme des Merisiers, 91191 Gif-sur-Yvette, France

³CAVELab Computational and Applied Vegetation Ecology, Department of Applied Ecology and Environmental Biology, Faculty of Bioscience Engineering, Ghent University, Coupure Links 653, 9000 Ghent, Belgium

⁴INRA, UMR EEF, 54280 Champenoux, France

Author for correspondence: Emilie Joetzjer (emilie.joetzjer@msu.montana.edu)

Abstract

We evaluate the ISBA_{CC} land surface model over the Amazon forest, and propose a revised parameterization of photosynthesis, including new soil water stress and autotrophic respiration functions. The revised version allows the model to better capture the energy, water and carbon fluxes when compared to five Amazonian fluxtowers. The performance of ISBA_{CC} is slightly site-dependent but similar to the widely evaluated land surface model ORCHIDEE, based on different assumptions. Changes made to the autotrophic respiration functions, including a vertical profile of leaf respiration, leads, to simulate yearly carbon use efficiency and carbon stocks consistent with an ecophysiological meta analysis conducted on three Amazonian sites. Despite these major improvements, ISBA_{CC} struggles to capture the apparent seasonality of the carbon fluxes derived from the fluxtower estimations. However, there is still no consensus on the seasonality of carbon fluxes over the Amazon, stressing a need for more observations as well as a better understanding of the main drivers of autotrophic respiration.

1. Introduction

The Amazon rainforest plays a crucial role in the regional energy, water and carbon cycles, thereby modulating the global climate system. The forest recycles about 25 to 35 % of the Amazonian precipitation through evapotranspiration (Eltahir et Bras, 1994) and stores about 10 to 15 % of the global above ground biomass (e.g. Potter and Klooster, 1999; Malhi et al., 2006; Beer et al. 2010; Pan et al., 2011). Despite intense deforestation and land use change, this region has acted as a long-term carbon sink (Phillips et al., 2008; Gatti et al., 2010; Gloor et al., 2012; Gatti et al., 2014; Espírito-Santo et al., 2014), meaning that the carbon uptake by photosynthesis exceeded on average, the carbon released by autotrophic respiration and decomposition.

Recent observations showed that the Amazon sink has already been weakened by environmental perturbations such as deforestation (Lewis et al., 2009; Aragao et al., 2014; Pan et al., 2011) and extreme droughts (Marengo et al., 2011; Gatti et al., 2014). Any change from sink to source of carbon would have profound impacts, including enhancement of global

50 warming through a positive carbon feedback loop (Foley et al., 2003; Cox et al., 2000; Huntingford et al., 2013). The response of the Amazon sink to the combined pressures of deforestation and climate change would be dramatic, especially as a majority of climate models project dryer and longer dry seasons at the end of the century (Fu et al., 2013; Joetzjer et al., 2013).

55 Given the strong coupling between climate and the carbon cycle and the emergence of holistic Earth System Models (ESM), modeling the Amazon rainforest is an important challenge. However, carbon balance projections are still highly uncertain, especially in the tropics (Friedlingstein et al., 2006; Jones et al., 2013; Anav et al., 2013; Huntingford et al., 2013).
60 Beyond the scenario of anthropogenic CO₂ emissions, key uncertainties are related to the carbon cycle response to a given scenario which depends on both model-dependent regional climate sensitivity (Berthelot et al., 2005; Alström et al., 2012) and model-dependent representation of carbon fluxes and stocks themselves (Dalmonech et al., 2014; Huntingford et al., 2013).

65 Most land surface models (LSMs) still struggle to capture the seasonal pattern of the net ecosystem carbon exchange (NEE) over the Amazon basin (Saleska et al., 2003; Baker et al., 2008; Verbeeck et al., 2011), which is defined as the difference between the carbon released by both heterotrophic (R_H) and autotrophic respiration (R_A) and taken up through
70 photosynthesis by Gross Primary Productivity (GPP). Recent model developments have focused on improving the seasonality of the simulated GPP, using an improved soil hydrology (Fisher et al., 2007; Baker et al., 2008; Grant et al., 2009), optimizing model's parameters (Verbeeck et al., 2011), or, and with more success, implementing new phenological processes (De Weirdt et al., 2012; Kim et al., 2012). Despite its major role in the carbon balance, less
75 attention has been paid to ecosystem respiration (R_{ECO}) (Atkin et al. 2014, Rowland et al., 2014). Ecosystem respiration is the sum of R_H and R_A and is the result of multiple contributions (roots, wood, leaves for R_A and litter, soil carbon for R_H) that are all influenced by several environmental factors (temperature, soil water content, microbial dynamics). Ecosystem respiration plays a major role in explaining inter-annual variability of NEE at
80 many forest ecosystems (Valentini et al., 2000; Saleska et al., 2003, Rowland et al., 2014).

In this paper, we evaluate the ISBA_{CC} (Gibelin et al., 2008) LSM over the Amazon forest using in situ measurements and propose an alternative parameterization of both photosynthesis and autotrophic respiration. Such a focus is justified not only because ISBA_{CC}
85 has never been really evaluated on tropical rainforests, but also because ISBA_{CC} has been recently implemented in the CNRM Earth System Model to participate in the forthcoming phases of CMIP (Coupled Model Intercomparison Project) and C4MIP (Coupled Climate Carbon Cycle Model Intercomparison Project). In CMIP3, some early ESMs projected a possible Amazon dieback (represented as the depletion of ecosystem carbon pools) at the end
90 of the 21st century (Cox et al., 2000; 2013; Huntingford et al., 2013). Such dramatic projections are however very uncertain, depending for instance on the projected change in precipitation and dry-season length (Good et al., 2013), on the response of forest water-use efficiency (Keenan et al., 2013), and therefore on the accuracy of the water and carbon stocks and fluxes simulated at the land surface.

95 Here we conduct a step by step evaluation of the ISBA_{CC} land surface model against in situ observations collected at five instrumental sites over the Amazon forest. To illustrate rather than really quantify model uncertainties, we also compare ISBA_{CC} to the ORCHIDEE LSM (Krinner et al., 2005), which is based on different assumptions for the representation of

100 photosynthesis, carbon allocation and growth. In section 2, we first briefly describe both
models and the available observations. In section 3, we propose alternative parameterizations
of photosynthesis and photosynthesis sensitivity to soil water stress and of autotrophic
respiration in ISBA_{CC}. In section 4, we compare the skill of the various ISBA_{CC}
105 parameterizations to capture the observed water and carbon fluxes and stocks. The main
conclusions are summarized in section 5.

2. Material and method

2.1 Observations

110 To evaluate carbon and water fluxes over the Amazon tropical forest, we use field
measurements of five eddy flux towers in Amazonia. Four towers are located in Brazil and
were established during the LBA (Large Scale Biosphere atmosphere) project (Da Rocha et
al., 2009): Manaus km 34 (M34), Santarem km 67 (K67) and 83 (K83), Reserva Jaru (JRU).
115 The fifth tower is the Gyaflux tower (GFG) located at Paracou in French Guiana (Bonal et
al., 2008). At JRU the forest is a semi-deciduous forest, whereas the other sites are
representing typical tropical rainforests. Site location is shown in figure 1 together with the
corresponding monthly mean climatologies of temperature and precipitation. Large seasonal
variations in precipitation are found at GFG and JRU, the two wettest sites, in contrast with
120 the other sites. Most datasets can be downloaded from the LBA website. For a detailed
description of each site, please refer to the literature indicated in Table 1 or to Costa et al.
(2010) and Baker et al. (2013) for a comparative analysis of the Brazilian sites.

For each site, meteorological forcings, such as incoming solar and infrared radiations,
125 precipitation (P), temperature (T) and specific humidity, are recorded every 30 minutes above
the canopy. Observations also include turbulent sensible (H) and latent heat (LE) fluxes and
net ecosystem carbon exchange (NEE) measured using the eddy-covariance method
(Shuttleworth et al., 1984; Aubinet et al., 2000; Baldocchi et al., 2001). Further information
on data acquisition and pre-processing can be found in the references indicated in Table 1.
130 Note that evaluation scores are here computed only against the more reliable daytime
measurements (Aubinet et al., 2002). At K83, measurements of soil moisture were collected
in two adjacent soil pits which are 10-m deep (Bruno et al., 2006) and 2-m deep (da Rocha et
al., 2004) respectively.

135 Gross Primary Productivity (GPP) and carbon released by the whole ecosystem respiration
(R_{ECCO}) were retrieved from NEE data using the Reichstein et al. (2005) algorithm. However, it
does not give any information either on the partitioning between autotrophic (R_A) and
heterotrophic (R_H) respiration, or on carbon allocation to canopy, wood and roots. Yet, these
are essential processes to correctly represent the functioning of the Amazon ecosystem (Malhi
140 et al., 2011). Malhi et al. (2009) gathered ecological measurements from K67, M34 and
Caxiuanã (1.72°S 51.46°W, Eastern amazon) to evaluate yearly average carbon cycling and
allocation. We here use this dataset to evaluate the annual carbon fluxes (GPP, R_A, NEE), the
carbon stocks and the carbon allocation between the different pools in ISBA_{CC} (section 4.4).

145 Finally, flux data are noisy. Hollinger et Richardson (2005) evaluated the relative uncertainty
of H, LE and CO₂ fluxes to be around 25 % on a temperate site. Energy balance closure in
eddy covariance data can also be problematic. At the five sites considered here, the overall
energy balance ratio calculated as the sum of (LE + H) divided by the sum of net radiation
over the whole period (Wilson et al., 2002) varies between 0.69 at M34 and 1.008 at K67,

150 with values of 0.79 at JRU, 0.87 at K83 and 0.96 at GFG. Energy balance would be achieved
with a ratio of one. For the carbon fluxes, according to Desai et al. (2008), the flux
partitioning method to retrieve GPP and R_{ECO} from NEE may add up to 10 % uncertainty.
Despite these uncertainties, eddy flux measurements are for now the best way to investigate
155 fluxes between the vegetation and the atmosphere especially when combined with ecological
measurements like those gathered by Malhi et al. (2009).

2.2 Models and experimental design

ISBA_{CC} (Interaction Soil Biosphere Atmosphere Carbon Cycle, Noilhan et Planton, 1989;
160 Noilhan et Mahfouf, 1996) and ORCHIDEE (Organizing Carbon and Hydrology In Dynamic
Ecosystems-version 1187) LSMs compute the exchange of water, energy and carbon between
the land surface and the atmosphere. Both models deal with photosynthesis and allocate
photosynthetic assimilates in several living biomass carbon pools defined by histological
functional type. In both models each carbon pool is associated with a respiration function and
165 a specific turnover rate. None of these two models take into account demography.

Carbon assimilation and allocation in the biomass pools differ greatly between the two
models. In ORCHIDEE, carbon assimilation is based on the leaf-scale equation of Farquhar et
al., (1980) for C_3 plants and is assumed to scale from leaf to canopy with APAR decreasing
170 exponentially with leaf area index (LAI), according to the “big leaf” approximation. Stomatal
conductance is proportional to the product of net CO_2 assimilation by atmospheric relative
humidity divided by atmospheric CO_2 concentration in the canopy (Ball et al., 1987).
Standard equations are given in Krinner et al. (2005), and Verbeeck et al. (2011) for tropical
forest plant functional types. In contrast, ISBA_{CC} has a semi-empirical parameterization of net
175 carbon assimilation and the mesophyll conductance (g_m) following the model of
photosynthesis proposed by Jacobs (1994), based on Goudriaan et al. (1985) and implemented
by Calvet et al. (1998). In its standard version, ISBA_{CC} uses Goudriaan’s (1986) solution of
radiative transfer to calculate net photosynthesis in 3 canopy layers. The standard ISBA_{CC}
equations are given in Calvet et al. (1998, 2004) and Gibelin et al. (2008). In
180 ORCHIDEE(v1187), the carbon allocation model accounts for 8 biomass compartments
(leaves, roots, fruits/harvested organs, reserves, aboveground sapwood, belowground
sapwood, aboveground heartwood, belowground heartwood) for tree plant functional types.

ISBA_{CC} represents aboveground metabolic and structural biomass pools, above and below
185 ground woody biomass pools and below ground structural biomass pool adapted from
Lemaire and Gastal (1997), implemented in ISBA_{CC} by Calvet and Soussana (2001) and
detailed in section 3.3. The description of the litter and soil carbon content and the associated
heterotrophic fluxes is similar between the two models and is based on the CENTURY model
developed by Parton et al. (1988). We only use the first top meter of soil carbon from the
190 dataset of Malhi et al. (2009) to evaluate ISBA_{CC} since CENTURY was designed to represent
the carbon content in the first top meter. The litter is described by 4 pools defined by the
lignin content and the location (metabolic and structural above and below ground). The soil
organic cycling module differentiates 3 carbon pools (active, slow, passive) according to their
turnover times (from a few years for the active pool to 1200 years for the passive pool).

195 At each site, we ran ISBA_{CC} and ORCHIDEE offline forced by in situ hourly meteorological
measurements (gap filled when necessary) made on top of each flux tower (available at
"http://beija-flor.onrl.gov/lba", except for GFG, available from the fluxnet website following
the “LaThuile” data sharing policy). We imposed the same evergreen tropical broadleaf tree

200 plant functional type at the 5 sites and used the in situ soil texture, root and soil depth
information for each site found in the literature and summarized in Table 1. Soil texture is
used to compute the wilting point and field capacity, and the hydrological and thermal
exchange coefficients following Decharme et al. (2011). The organic content in the upper soil
205 layers, which also affects the hydrological and thermal exchange coefficients, is given by
HWSD (Harmonized World Soil Database, Nachtergaele et al., (2012)). Both models were
run until the slowest storage pools had reached equilibrium by cycling the atmospheric
forcing over the available 3 years including the observed CO₂ concentration. To simulate soil
moisture content in the deep Amazonian soils we used the soil multilayer diffusion scheme
implemented in ISBA by Decharme et al. (2011, 2013) and in ORCHIDEE by de Rosnay et
210 al. (2000, 2002). Both models impose a vertical distribution of roots following a decreasing
exponential function of depth.

3. Towards a new parameterization of the tropical forest in ISBA_{CC}

215 ISBA_{CC} has never been evaluated over the tropical rainforest biome (Gibelin et al., 2008), and
as shown below, in this control version (CTL), LE and R_A were seriously biased and needed
to be corrected. Large biases in the simulated latent heat and respiration fluxes are indeed not
acceptable when modelling a region where precipitation recycling is important and where
changes in the carbon fluxes could have profound effects on the global climate. This section
220 describes the original ISBA_{CC} model (CTL) and the implemented modifications. The main
parameters of ISBA_{CC} are given in Table 2. We first describe the changes made on the
photosynthesis parameterization and its sensitivity to soil moisture as summarized in Table 3.
Second, we present the modified autotrophic respiration functions (version PS+R) and the
original ones (CTL) as summarized in Table 4.

225

3.1 ISBA_{CC}; selection of the reference version

As pointed out by Carrer et al. (2013), ISBA_{CC} overestimates Gross Primary Productivity
(GPP) at global scale, and especially in the tropical forests where the original radiative
230 transfer code (Calvet et al., 1998) resulted in too high available radiation. Carrer et al. (2013)
proposed a new radiative transfer scheme, dividing the canopy in 10 layers and accounting for
the effect of direct and diffuse light and for sunlit and shaded leaves. As illustrated in figure 2
for the K67 site, the original radiative transfer scheme greatly overestimates the GPP at hourly
and seasonal time scales. The other sites have a similar behavior (not shown). The new
235 version of the radiative transfer allows ISBA_{CC} to better capture the amount of GPP thanks to
a more detailed and physical approach. To avoid unrealistic GPPs, we chose to test the
version of ISBA_{CC} with Carrer et al.(2013) radiative transfer scheme and call it our control
version (CTL).

240 3.2 Water and carbon coupling and drought sensitivity: description of the original and modified parameterization (PS version)

The original ISBA_{CC} photosynthesis model relies on a “mesophyll conductance” (g_m), defined
by Jacobs (1994) as the initial slope of the CO₂ response curve at high light intensity and
245 limiting CO₂ concentrations.

$$g_m = \frac{A_m}{C_i - \Gamma} \quad (1)$$

250 with C_i the leaf-internal CO₂ concentration, Γ the CO₂ compensation point and A_m the photosynthesis rate at saturating light and low C_i .

The model also supposes a constant ratio of C_i to atmospheric CO₂ concentration (C_a) when atmospheric humidity is constant.

$$255 \quad f = \frac{C_i - \Gamma}{C_a - \Gamma} \quad (2)$$

In drier atmospheric conditions, the ratio decreases according to:

$$f = f_0 \left(1 - \frac{D_s}{D_{max}} \right) + f_{min} \left(\frac{D_s}{D_{max}} \right) \quad (3)$$

260 where D_s is the atmospheric humidity deficit, D_{max} the deficit resulting in complete stomatal closure, f_{min} the value of f at D_{max} , and f_0 the value of f at saturating humidity ($D_s = 0$). f_{min} , f_0 and D_{max} are model parameters depending on plant type and based on available observations. Following eq. (2), C_i also decreases with drying air (increase in D_s):

$$265 \quad C_i = f \cdot C_a + \Gamma(1 - f) \quad (4)$$

Assimilation is then calculated from light (eq. A7 - A9 in Calvet et al., 1998), air humidity, C_a , the ratio of C_i / C_a and finally, the stomatal conductance (g_s) is deduced from the assimilation rate.

270 Jacobs (1994) photosynthesis model was designed to simulate the assimilation rate and the stomatal conductance of grapevines in semi arid conditions. While ISBA_{CC} is used for large scale studies using a PFT (Plant Functional Type) approach, there were few attempts to adapt the ecophysiological parameters to each functional group, especially for evergreen tropical broadleaf trees. We used published measurements from about 20 different tree species (Domingues et al., 2005, 2007) from Tapajos National forest to derive $A_{m,max}$, the maximum photosynthesis rate at high light intensity and f_0 (see eq. 3). The original values and the values of these two parameters are given in Table 3.

280 The soil water stress function (WSF) empirically describes the effect of soil moisture on transpiration and photosynthesis. In the case of ISBA_{CC}, soil water content (SWC) weighted by the roots profile, affects transpiration and photosynthesis through changes in g_m and, in the CTL version, f_0 . The WSF implemented in ISBA_{CC} by Calvet (2000) was first designed for herbaceous species and adapted for trees (Calvet et al., 2004). As described in Table 3 the parameterization for trees supposes a relationship between f_0 and soil wetness index (SWI) and was derived from measurements taken on saplings from *Pinus pinaster* and *Quercus petraea*. It had never been tested on mature trees and tropical species and doesn't perform well when tested in the Amazon as shown below. Therefore, we propose an alternative parameterization assuming a constant f_0 coherent with in situ observations (Domingues et al., 2007) and validated against the two artificial droughts experiments lead in the eastern Amazon (Joetzjer et al., 2014, and references within). Further in this paper, we call version PS, ISBA_{CC} version with these different values of $A_{m,max}$, f_0 and the modified WSF.

295 **3.3 Autotrophic respiration and specific leaf area : description of the original and**
300 **modified parameterization (PS+R version)**

An analysis of the yearly carbon use efficiency (CUE) defined by the fraction of GPP invested into the Net Primary productivity (NPP/GPP) (Rowland et al., 2014) shows that ISBA_{CC} overestimates R_A from leaves, roots and wood, leading to a loss of more than 90 % of the carbon assimilated on an annual basis (corresponding to a CUE < 0.1). This result is not realistic. Over the Amazon, the CUE is roughly estimated to be around 0.3 (Chambers et al., 2004; Malhi et al., 2009, 2011; Metcalfe et al., 2010). Therefore, a new parameterization of each respiration term is proposed and described below.

305 ISBA_{CC} simulates 6 biomass pools, originally described in Gibelin et al. (2008) as:

- leaf biomass (B_l)
- B2, an active structural biomass pool which represents the stem in the case of grass and crop, and can be assimilated to new twigs for trees.
- B3, a small biomass pool used for numerical stability purposes, and accounts for a negligible amount of the carbon actually stored.
- B4, a below ground structural biomass pool representing the roots's sapwood and the fine roots.
- 315 - B5, an above ground woody biomass pool representing the above ground wood (trunk and branches).
- B6, a below ground woody biomass pool representing the roots's heartwood.

The evolution of each biomass pool B (kg m^{-2}) is given by:

320
$$\frac{\Delta B}{\Delta t} = A_B - D_B - R_B \quad (5)$$

where $\Delta t =$ one day, A_B ($\text{kg m}^{-2} \text{ day}^{-1}$) is the increase in biomass coming from photosynthetic assimilation or allocation from another reservoir, D_B ($\text{kg m}^{-2} \text{ day}^{-1}$) represents turnover or carbon reallocation to another pool, and R_B ($\text{kg m}^{-2} \text{ day}^{-1}$) is a decrease term due to respiration.

3.3.1 Leaf respiration

330 Originally, leaf dark respiration integrated over the canopy was parameterized, following Van Heemst (1986) as:

$$R_{leaf} = \frac{A_m}{9} \cdot LAI \quad (6)$$

335 with LAI the Leaf Area Index and A_m , the photosynthetic rate at high light intensities (Table 1). A_m being constant throughout the canopy, respiration is identical from the top to the bottom leaves, while assimilation decreases from top to bottom according to the absorbed fraction of PAR calculated by the radiative transfer scheme (Carrer et al., 2013). However, observations show that leaf respiration is positively correlated to area based leaf nitrogen content (N_{AREA}) (Meir et al., 2001; Reich et al., 2006; Meir et al., 2008), and N_{AREA} is driven by light availability according to the theory of optimal nutrient allocation availability (Field et Mooney, 1986). Indeed, N_{AREA} is highly correlated to photosynthesis capacity as most of the leaf nitrogen is dedicated to the synthesis of photosynthetic proteins. So, a constant value for

345 dark respiration throughout the canopy as supposed in ISBA_{CC} is not reasonable, particularly for high canopies. Therefore we imposed a vertical profile of respiration based on an exponential profile of leaf nitrogen (section 2.5 Bonan et al., 2011, 2012).

$$R_{leaf} = \frac{A_m}{9} \cdot \exp(-k_n \cdot LAI) \quad (7)$$

350 With k_n the within-canopy profile of photosynthetic capacity set to 0.2 according to Mercado et al. (2009) and Bonan et al. (2011). This parametrization greatly reduces the leaf dark respiration of the canopy compared to the original one.

3.3.2 Twigs, stem and trunk

355 In the original version of ISBA_{CC} (Gibelin et al., 2008) the woody biomass (B5) does not respire. If heartwood does not respire, sapwood made of living cells (including phloema cells) does. We adopted the simple parameterization of sapwood respiration from IBIS (Kucharik et al., 2000). We first calculate an estimated sapwood fraction (λ_{sap}) from an assumed sap velocity, the maximum transpiration rate and the tree height following Kucharik et al. (2000).
360 Then, the respiration of the 5th reservoir, R_5 is computed as:

$$R_5 = B_5 \cdot \lambda_{sap} \cdot \beta_{wood} \cdot f(T) \quad \text{with } \beta_{wood} = 0,0125 \text{ yr}^{-1} \quad (8)$$

365 where β_{wood} is a maintenance respiration coefficient defined at 15°C and $f(T)$ is given by the Arrhenius temperature function modified by Lloyd et Taylor, (1994).

$$f(T) = \exp \left[E_o \left(\frac{1}{15 - T_0} \right) - \frac{1}{T - T_0} \right] \quad (9)$$

370 with T the temperature of the given carbon pool in °C (here, the surface temperature because ISBA_{CC} doesn't simulate a vegetation temperature), E_o a temperature sensitivity factor (*equal to 3500*) and T_0 a temperature reference set at 25°C.

For the B2 biomass reservoir, (twigs), the function proposed in ISBA_{CC} is:

$$375 \quad R_2 = B_2 \cdot \eta \cdot Q_{10}^{\frac{T_s - 25}{10}} \quad (10)$$

380 where $Q_{10}=2$ and $\eta = 0.01$ (g g⁻¹ day⁻¹) and T_s (°C) the temperature of the surface. We didn't find any measurement for respiration of twigs and didn't find any other model representing this reservoir. We assumed that respiration per unit biomass of this reservoir had to be lower than respiration of leaves, and similar or slightly larger than sapwood. A comparison with respiration functions from other models showed that (10) is about the same magnitude as respiration functions for leaves from ORCHIDEE, LPJ (Sitch et al., 2003) and IBIS (Foley et al., 1996) for temperatures up to 30°C but increases strongly at higher temperatures. It is also an order of magnitude larger than respiration of sapwood from these models, which doesn't
385 seem realistic. To be coherent with B5, we adopted Kucharik et al. (2000) formulation. Therefore:

$$R_2 = B_2 \cdot \beta \cdot f(T) \text{ with } \beta = 1.25 \text{ y}^{-1} \quad (11)$$

390 3.3.3 Root respiration

Originally, root respiration followed the linear respiration given in Ruimy et al. (1996):

$$R_4 = B_4 \cdot R_0 (1 + 0.16 T_p) \text{ with } R_0 = 1.9 \cdot 10^4 \text{ g g}^{-1} \text{ day}^{-1} \quad (12)$$

395

To be consistent with sapwood respiration, R_4 is now computed as:

$$R_4 = B_4 \cdot \beta \cdot f(T) \text{ with } \beta = 1.25 \text{ y}^{-1} \quad (13)$$

400

3.3.4 Specific Leaf Area

ISBA_{CC} calculates interactively the leaf biomass and the Leaf Area Index (LAI) using a simple growth model (Calvet et al., 1998). Leaf biomass results directly from the carbon balance of the leaf: increasing with the carbon assimilated by photosynthesis and depleted by respiration, turnover, and allocation to the other reservoirs (Calvet and Soussana, 2001). LAI is simply calculated as leaf biomass times the Specific Leaf Area (SLA). Hence there is no explicit phenology model in ISBA_{CC}. Phenology is simply the result of the leaf carbon balance.

410 In the CTL version the SLA depends on the leaf nitrogen concentration, a fixed parameter depending on the plant type (Gibelin et al., 2006). We replaced the original SLA calculated by Gibelin et al. (2006) by the observed value from Domingues et al. (2007).

415 Further in this paper, we call version PS+R, ISBA_{CC} version including the Table 3 parameters and functions, and the changed autotrophic respiration and SLA summarized Table 4.

4. Results and discussion

420 We now evaluate and compare three versions of ISBA_{CC}: CTL, PS and PS+R described in section 3.1, 3.2 and 3.3 respectively. We illustrate the uncertainties linked to the choice of model by showing the fluxes simulated by the well evaluated ORCHIDEE (v.1187) land surface model over the same sites. Note that we mostly show results from K83 because deep soil moisture measurements are available.

425 4.1 Soil moisture

Looking at the top-10m daily soil water content simulated in 2003 at K83 (Fig. 3, bottom panel), the slight wet bias found in the original ISBA_{CC} model (CTL) is reduced when using either the modified PS or PS+R versions. As shown in section 4.2, this is due to the increased LE in the PS and PS+R versions. Note that the ISBA_{CC} soil moisture content was also successfully evaluated at K67 and at Caxiuana (Joetzjer et al., 2014, fig 3 top panels). Moving to the vertical profile of soil moisture (Fig. 3 mid panels), and whatever the model version, the vertical profile of organic matter prescribed in ISBA_{CC} (Decharme et al., 2006) allows the model to simulate a relatively wet top-1m horizon as observed (Fig. 3 mid panels). However, it is not sufficient to capture accurately the observed soil moisture dynamics. From February to April the soil moisture increases slowly from the surface to 6 meters while ISBA_{CC}

435

440 simulates a much more rapid re-wetting, and after a heavy rain (e.g October) water infiltrates too quickly. This might be due to uncertainties in water uptake by roots (prescribed according to Jackson et al, 1996), but also to the vertically uniform soil texture prescribed in ISBA_{CC} due to the lack of in situ observations. In reality, the clay content is usually increasing with depth, which reduces the hydraulic conductivity at lower levels.

4.2 Energy Budget

445 Focusing again on K83, while net radiation (R_{net}) is well captured by the three ISBA_{CC} simulations, the CTL experiment overestimates the sensible heat flux (H) and underestimates the latent heat flux (LE) (Fig. 4). As expected, the partitioning of the energy budget is better represented with the simulation using $A_{m,max}$ and f_0 parameters derived from the in situ observations (PS version, Table 3). The increase in LE simulated by PS compared to the CTL
450 explains the reduction of the wet bias in SWC simulated by the CTL run (Fig. 3). Not surprisingly, the modification of the autotrophic respiration functions has little effect (run PS+R, Table 4) on the simulated energy budget and does not impact the temporal variability of R_n , H and LE which are reasonably well simulated at both diurnal and seasonal time scales.

455 Figure 5 shows a summary of the annual mean scores of H and LE computed for the three versions of ISBA_{CC} and for ORCHIDEE at the five flux towers using Taylor diagrams and a comparison of biases relative to the model mean climatology. Taylor plots are polar coordinate displays of the linear correlation coefficient and centered root mean square error (RMSE, pattern error without considering bias) between the simulated and observed fields,
460 and the ratio of their standard deviations (Taylor, 2001). Correlations mainly reflect the diurnal cycle and are reasonable (above 0.6). The PS (and PS+R) parameterizations barely impact correlations and slightly improve the root mean square error (RMSE) compared to the CTL. However, the standard deviation is improved for all sites compared to the CTL runs.
465 The CTL runs show a systematic overestimation of H (positive bias, fig 5, bottom panel) that is strongly reduced in both PS and PS+R versions. Conversely, LE is greatly underestimated (by about 30 %) by CTL, whatever the season (not shown), at four among the five sites and this bias is reduced in the revised versions. At M34, although CTL overestimates H, it simulates reasonably well LE. The PS model version reduces the bias in H but overestimates
470 LE. This result is coherent with the fairly low level of energy closure at this site (see section 2.1) and suggests that the observed Bowen ratio should be considered with caution at M34.

The PS version improves the simulation of H and LE compared to the CTL version, whatever the season. Interestingly, changes in the parameterization of respiration (PS+R) barely alter
475 the results compared to PS. The scores of ORCHIDEE are very close to those computed with the improved version of ISBA_{CC} with large positive biases for H at JRU and LE at M34 (Fig. 5). The fact that the results are more site-dependent than model-dependent suggests a problem in the prescribed atmospheric forcings or in the eddy-covariance measurements for these sites, as suggested by the level of energy closure on these sites. The ISBA_{CC} and ORCHIDEE
480 models being based on different parameterizations of photosynthesis, respiration and growth, the likelihood of the models being both wrong at the same location is rather small, except for processes unaccounted for by both models, like particular phenology adapted to the local conditions.

485

4.3 Carbon fluxes

Moving back to the K83 site, but looking at the carbon fluxes (Fig. 6), the ISBA_{CC} model reasonably captures the annual amount of carbon taken up by photosynthesis (GPP), released by respiration (R_{ECO}) and the net flux defined in the model as the difference between R_{ECO} and GPP (NEE). The annual magnitude of GPP is correctly simulated by the CTL version thanks to the radiative transfer scheme proposed by Carrer et al. (2013) (Fig. 2). While the $A_{m,max}$ chosen in the PS simulation is around six times smaller than initially (Table 3), the increase in f_0 enhances the assimilation rate, leading to little change in GPP between CTL and PS. So, there is a trade-off in the model between f_0 and $A_{m,max}$, that can be expected from the photosynthesis module. A lower maximum assimilation rate ($A_{m,max}$) tends to reduce the carbon assimilation (see eq. A7 in Calvet and Soussana, 2001). On the other hand, with a higher f_0 , intracellular CO_2 is higher (see equation 4), which favors carbon assimilation. PS barely impacts simulated R_{ECO} and therefore NEE compared to CTL. While the revised SLA and respiration functions lead to slightly decreased GPP (PS+R), the decrease in R_{ECO} is even stronger and leads to an increased net rate of carbon uptake (more negative NEE).

The annual cycle of GPP, R_{ECO} and NEE, although relatively small in these tropical regions (Fig. 6, right column), is poorly simulated by the model. The model tends to increase GPP at the beginning of the dry season when radiation increases and soil moisture is not yet limiting. As such, the model behaves as expected, radiation being the most limiting factor during the wet season, and the observed annual cycle results probably from processes that are not accounted for by the model, such as leaf phenology. Not surprisingly given the model formulation, but in contrast to the observations, the modelled seasonal cycle of GPP coincides with the seasonal cycle of LE in all ISBA_{CC} simulations.

The statistical skill scores computed for the five flux towers are again summarized in Taylor diagrams (Fig. 7, top). The GPP relative standard deviation (RSD) computed with PS is improved at K67 but is slightly lowered at M34, while there are no substantial changes at K83 and JRU compared to CTL. This is also valid for the NEE. At GFG, the RSD of NEE is also improved. PS+R exhibits scores quite similar to the PS run. The systematic positive bias in GPP (about 10 to 25 %) and in R_{ECO} (about 10 to 100 %) found in the CTL run is reduced in PS, and even more in PS+R (Fig. 7, bottom). Although model modifications reduce the bias in NEE at JRU and M34, they increase it at K67, K83 and GFG. This is not surprising since NEE is a small flux resulting from the difference between two large fluxes. Looking at the absolute RMSE, errors are reasonable (between 5 and 10 $\mu\text{mol m}^{-2} \text{s}^{-1}$) compared to observation uncertainties and ORCHIDEE's results once again suggest that scores are more site-dependent than model-dependent.

It is important to note that flux towers measure directly only NEE. The R_{ECO} is reconstructed from nighttime (i.e. when there is no photosynthesis) measurements which are however questionable (e.g. Reichstein et al., 2005). Daytime R_{ECO} is likely to differ from nighttime R_{ECO} because of the temperature diurnal cycle. Also, the lower wind speed at night and thus lower friction velocity (u^*) limits the efficiency of the eddy-covariance technique (Aubinet et al., 2002; Saleska et al., 2003). As GPP is reconstructed from NEE and R_{ECO} , more bias can be expected for this flux and conclusions on GPP should be also considered with caution.

4.4 Carbon Stocks and carbon use efficiency

The data compilation of Malhi et al. (2009) at Caxiuanã, K67 and M34 provides valuable insights to evaluate the model ability to simulate the annual carbon storage per carbon pools

(Fig. 8). While there are few differences between the CTL and PS+R simulations in terms of GPP and R_{ECO} , the carbon stocks greatly differ (Fig. 8). Over these three sites, observations indicate a total carbon stock around 330 tC ha^{-1} with an error estimate of about 30 tC ha^{-1} . The original model (CTL) greatly underestimates the stock by a factor of three. While modifications of the photosynthesis components (PS) slightly increases carbon stocks, the underestimation of the carbon storage persists. Changes in respiration functions (PS+R) lead to a more reasonable total amount of carbon stock.

Flux tower data provide high frequency information on the carbon flux between the ecosystem and the atmosphere, but do not allow us to distinguish between vegetation and soil fluxes. The meta analysis from Malhi et al. (2009) however allows us to evaluate the annual fluxes between the different carbon pools at Caxiuanã (Fig. 9). Compared to observations, the CTL run highly overestimates R_A and consequently underestimates the NPP. Therefore, the Carbon Use Efficiency (CUE), computed as the ratio NPP/GPP , is too low. 92 % of the carbon assimilated is directly respired, leaving only 8 % of the GPP to be allocated to the plant biomass pools. This result motivated the changes in autotrophic respiration functions presented in Table 4. These changes (simulation PS+R, Table 4) lead to a more realistic CUE (around 0.3; e.g. Malhi et al. 2009; Rowland et al. 2014.), therefore enhancing the carbon storage in the leaf, wood and root pools, and the litterfall. The litter and the soil organic matter are increased, and, as a result, heterotrophic respiration, largely underestimated by the original model (CTL), is now correctly simulated. Note that the CTL version has a reasonable estimation of R_{ECO} because the overestimation of R_A is partly counterbalanced by an underestimation of R_H through an underestimation of the heterotrophic carbon stock (Fig. 9).

In spite of reasonable R_A at each site, the ISBA_{CC} model tends to overestimate the amount of carbon stored in the stems (Fig. 8). This pattern can very likely be explained by a too low mortality rate. At K67, the high amount of coarse and woody debris (Saleska et al., 2003) and the low amount of above ground biomass observed compared to the other sites suggest a recent higher than normal tree mortality. This could be triggered by drought associated with the strong El Niño events of the 1990s (Rice et al., 2004; Pyle et al., 2008) that these simulations forced by 3 years meteorological forcing cannot represent.

4.5 Annual ratio between carbon stocks and fluxes

The ratio of respiration of a particular pool relative to its size is particularly instructive (Table 5) to evaluate the representation of the respiration process in the model. As can be seen at Caxiuanã, K67 and M34, about 10 % of the carbon stored in the plants is respired annually and between 7 and 9 % of the litter and soil carbon content, depending on the site. As a whole, about 9 % of the total biomass (soil, litter and plant) is respired. These percentages are very well captured by the new (PS+R) version but totally misrepresented by the original scheme (CTL). Ecosystem respiration relative to the stock is three times too high although the absolute value was reasonable. Nevertheless, large uncertainties surrounds the seasonality of R_A (and consequently R_{ECO}).

5. Conclusions

In this study, we proposed and evaluated revised parameterizations of the photosynthesis, its sensitivity to soil water stress and the autotrophic respiration function in the ISBA_{CC} land surface model implemented in the CNRM ESM, over the Amazon forest. As far as the energy and water budgets are concerned, net radiation and soil water dynamics that are driven by

observed atmospheric forcing are reasonably well simulated by ISBA_{CC}. Our modifications of photosynthesis mainly allow the model to better capture the turbulent energy fluxes (H and LE). While the mean carbon fluxes are slightly better captured with the revised parameterization, ISBA_{CC} still struggles to capture the seasonality of the observed (NEE) or reconstructed (R_{ECO} and GPP) carbon fluxes. Interestingly, when ISBA_{CC} is compared to the ORCHIDEE model based on different parameterizations, scores are systematically more site-dependent than model-dependent. This either suggests problems in the prescribed atmospheric forcing, or in the eddy-covariance measurements, unless both models do not account for a crucial process. Further investigations are thus needed.

Changes made to the parameterization of R_A improve the simulation of the Carbon Use Efficiency, in good agreement with the observations from Malhi et al. (2009) and Rowland et al. (2014). By enhancing the carbon storage, biomass pools become larger and more consistent with observations. However, increasing the carbon stock in ISBA_{CC} by a factor of three between CTL and PS+R versions barely impacts the net carbon flux. This illustrates the weak link between carbon stocks and fluxes in the ISBA_{CC} model and the need for further improvements.

There is no silver bullet for the parameterization of autotrophic respiration, such as the Farquhar model for the carbon assimilation. Because R_A represents a large part of R_{ECO} , and R_{ECO} is crucial to determine the net carbon balance (NEE), both annual amount and seasonality of R_A need to be correctly represented. Indeed, considering the relevance of R_{ECO} in the seasonal changes of the ecosystem carbon budget (Meir et al., 2008; Rowland et al., 2014), and not only over the Amazon forest (Atkin et Macherel, 2009; Atkin et al., 2014), there is an urgent need to better understand the main drivers of autotrophic respiration in a wide range of environmental conditions.

Acknowledgments

Thanks are due to the two anonymous reviewers for their constructive comments.

References

- Ahlström, A., Schurgers, G., Arneeth, A., and Smith, B.: Robustness and uncertainty in terrestrial ecosystem carbon response to CMIP5 climate change projections, *Environ. Res. Lett.*, 7, 044008, doi:10.1088/1748-9326/7/4/044008, 2012.
- Anav, A., Friedlingstein, P., Kidston, M., Bopp, L., Ciais, P., Cox, P., Jones, C., Jung, M., Myneni, R., and Zhu, Z.: Evaluating the land and ocean components of the global carbon cycle in the CMIP5 Earth System Models, *J. Clim.*, 26, 6801–6843. 2013.
- Aragao, L. E., Poulter, B., Barlow, J. B., Anderson, L. O., Malhi, Y., Saatchi, S., Phillips, O. L.; Gloor, E: Environmental change and the carbon balance of Amazonian forests. *Biological Reviews* 2014. .
- Araujo, A., Nobre, A., Kruijt, B., Elbers, J., Dallarosa, R., Stefani, P., von Randow, C., Manzi, A., Culf, A., Gash, J., Valentini, R., and Kabat, P.: Comparative measurements of carbon dioxide fluxes from two nearby towers in a central Amazonian rainforest: The Manaus LBA site, *J. Geophys. Res.*, 107, 58.1–58.20, 2002.

- Atkin, O. K. and Macherel, D.: The crucial role of plant mitochondria in orchestrating drought tolerance, *Ann. Bot. London*, 103, 581–597, 2009.
- 640 Atkin, O. K., Meir, P. and Turnbull, M. H. : Improving representation of leaf respiration in large- scale predictive climate–vegetation models. *New Phytologist*, 202(3), 743-748. 2014.
- Aubinet, M., Grelle, A., Ibrom, A., Rannik, U., Moncrieff, J., Foken, T., Kowalski, A. S., Martin, P., Berbigier, P., Bernhofer, C., Clement, R., Elbers, J., Granier, A., Grunwald, T., Morgenstern, K., Pilegaard, K., Rebmann, C., Snijders, W., Valentini, R., and Vesala, T.: Estimates of the annual net carbon and water exchange of forests: The Euroflux methodology, *Adv. Ecol. Res.*, 30, 113–175, 2000.
- 645 Aubinet, M., Heinesch, B., Longdoz, B.: Estimation of the carbon sequestration by a heterogeneous forest: night flux corrections, heterogeneity of the site and inter-annual variability. *Glob. Change Biol.* 8, 1053–1097. 2002.
- Baldocchi, D., Falge, E., Gu, L., Olson, R., Hollinger, D., Running, S., Anthoni, P., Bernhofer, C., Davis, K., Evans, R., Fuentes, J., Goldstein, A., Katul, G., Law, B., Lee, X., Malhi, Y., Meyers, T., Munger, W., Oechel, W., Paw U, K. T., Pilegaard, K., Schmid, H. P., Valentini, R., Verma, S., Vesala, S., Wilson, K., Wofsy, S.: FLUXNET: A new tool to study the temporal and spatial variability of ecosystem-scale carbon dioxide, water vapor, and energy flux densities. *Bulletin of the American Meteorological Society*, 82(11), 2415-2434. 2001.
- 655 Ball, J. T., Woodrow, I. E., and Berry, J. A.: A model predicting stomatal conductance and its contribution to the control of photosynthesis under different environmental conditions, in: *Progress in Photosynthesis Research*, Vol. 4, edited by: Biggins, J., Martinus Nijhoff, the Netherlands, 221–224, 1987.
- 660 Baker, I. T., Prihodko, L., Denning, A. S., Goulden, M. L., Miller, S., and da Rocha, H. R.: Seasonal drought stress in the amazon: reconciling models and observations, *J. Geophys. Res.*, 113, 2005–2012, doi:10.1029/2007JG000644, 2008.
- 665 Baker, I. T., Harper, A. B., da Rocha, H. R., Denning, A. S., Araújo, A. C., Borma, L. S., Freitas, H. C., Goulden, M. L., Manzi, A. O., Miler, S.D., Nobre, A. D., Restro-Coupe, N., Saleska S. R., Stöckli, R., von Randow, C., Wofsy, S. C.: Surface ecophysiological behavior across vegetation and moisture gradients in tropical South America. *Agricultural and Forest Meteorology*, 182-183, 177–188. 2013.
- Beer, C., Reichstein, M., Tomelleri, E., Ciais, P., Jung, M., Carvalhais, N., Rodenbeck, C., Arain, M. A., Baldocchi, D., Bonan, G. B., Bondeau, A., Cescatti, A., Lasslop, G., Anders, L., Lomas, M., Luyssaert, S., Margolis, H., Oleson, K. W., Rouspard, O., Veenendaal, E., Viovy, N., Williams, C., Woodward, F. I., and Papale, D.: Terrestrial gross carbon dioxide uptake: global distribution and covariation with climate, *Science*, 329, 834–838, doi:10.1126/science.1184984, 2010.
- 675 Berthelot, M., Friedlingstein, P., Ciais, P., Dufresne, J.-L., and Monfray, P.: How uncertainties in future climate change predictions translate into future terrestrial carbon fluxes, *Glob. Change Biol.*, 11, 959–970, doi:10.1111/j.1365-2486.2005.00957.x, 2005.
- 680 Bonan, G. B., P. J. Lawrence, K. W. Oleson, S. Levis, M. Jung, M. Reichstein, D. M. Lawrence, and S. C. Swenson: Improving canopy processes in the Community Land Model version 4(CLM4) using global flux fields empirically inferred from FLUXNET data, *J. Geophys. Res.*, 116, G02014, doi:10.1029/2010JG001593.2011.
- 685 Bonan, G. B., Oleson, K. W., Fisher, R. A., Lasslop, G., and Reichstein, M.: Reconciling leaf physiological traits and canopy flux data: use of the TRY and FLUXNET databases in the Community Land Model version 4, *J. Geophys. Res.*, 117, G02026, doi:10.1029/2011JG001913, 2012.
- 690

- 695 Bonal, D., Bosc, A., Ponton, S., Goret, J. Y., Burban, B., Gross, P., Bonnefond, J. M., Elbers, J., Longdoz, B., Epron, D., Guehl, J. M., and Granier, A.: Impact of severe dry season on net ecosystem exchange in the neotropical rainforest of french guiana, *Glob. Change Biol.*, 14, 1917–1933, doi:10.1111/j.1365-2486.2008.01610.x, 2008.
- 700 Bruno, R. D., da Rocha, H. R., de Freitas, H. C., Goulden, M. L. and Miller, S. D.: Soil moisture dynamics in an eastern Amazonian tropical forest, *Hydrol. Process.*, 20, 2477–2489, doi:10.1002/hyp.6211. 2006.
- 705 Calvet, J. C., Noilhan, J., Roujean, J. L., Bessemoulin, P., Cabelguenne, M., Olioso, A., and Wigneron, J. P.: An interactive vegetation SVAT model tested against data from six contrasting sites, *Agr. Forest Meteorol.*, 92, 73–95, 1998.
- Calvet, J. C., Soussana J., F. : Modelling CO₂-enrichment effects using an interactive vegetation SVAT scheme, *Agr. Forest Meteorol.*, 108,129-152, 2001.
- 710 Calvet, J. C., Rivalland, V., Picon-Cochard, C., and Guehl, J. M.: Modelling forest transpiration and CO₂ fluxes response to soil moisture stress, *Agr. Forest Meteorol.*, 124, 143–156, 2004.
- 715 Carrer, D., Roujean, J. L., Lafont, S., Calvet, J. C., Boone, A., Decharme, B., Delire, C., and Gastellu-Etchegorry, J. P.: A canopy radiative transfer scheme with explicit FAPAR for the interactive vegetation model ISBA-A-gs: impact on carbon fluxes, *J. Geophys. Res.-Biogeo.*, 118, 1–16, doi:10.1002/jgrg.20070, 2013
- 720 Chambers, J.Q., Tribuzy, E.S., Toledo, L.C., Crispim, B.F., Higuchi, N., dos Santos, J., Araujo, A.C., Kruijt, B., Nobre, A.D. & Trumbore, S.E : Respiration from a tropical forest ecosystem: partitioning of sources and low carbon use efficiency. *Ecological Applications*, 14, S72–S88. 2004.
- 725 Costa, M. H., Biajoli, M. C., Sanches, L., Malhado, A. C. M., Hutyra, L. R., Da Rocha, H. R., Aguiar, R. G., De Araújo, A. C.: Atmospheric versus vegetation controls of Amazonian tropical rain forest evapotranspiration: Are the wet and seasonally dry rain forests any different? *Journal of Geophysical Research: Biogeosciences*, 115(4), 1–9. <http://doi.org/10.1029/2009JG001179>, 2010.
- 730 Cox, P. M., Betts, R. A., Jones, C. D., Spall, S. A., and Totterdell, I. J.: Acceleration of global warming due to carbon-cycle feedbacks in a coupled climate model, *Nature*, 408, 184–187, 2000.
- Cox, P. M., Pearson, D., Booth, B. B., Friedlingstein, P., Huntingford, C., Jones, C. D., & Luke, C. M. :Sensitivity of tropical carbon to climate change constrained by carbon dioxide variability. *Nature*, 494(7437), 341-344. 2013
- 735 Dalmonech, D., Foley, A. M., Anav, A., Friedlingstein, P., Friend, A. D., Kidston, M., Willeit, M. and Zaehle, S. : Challenges and opportunities to reduce uncertainty in projections of future atmospheric CO₂: a combined marine and terrestrial biosphere perspective. *Biogeosciences Discussions*, 11(2), 2083-2153. 2014
- 740 Decharme, B., Douville, H., Boone, A., Habets, F., and Noilhan, J.: Impact of an exponential profile of saturated hydraulic conductivity within the ISBA LSM: simulations over the Rhone basin, *J. Hydrometeorol.*, 7, 61–80, 2006.
- 745 Decharme, B., Boone, A., Delire, C., and Noilhan, J.: Local evaluation of the Interaction between Soil Biosphere Atmosphere soil multilayer diffusion scheme using four pedotransfer functions, *J. Geophys. Res.*, 116, 1984–2012, 2011.

- Decharme, B., Martin, E., and Faroux, S.: Reconciling soil thermal and hydrological lower boundary conditions in land surface models, *J. Geophys. Res.-Atmos.*, 118, 1–16, 2013.
- 750 Desai, A. R., Richardson, A. D., Moffat, A. M., Kattge, J., Hollinger, D. Y., Barr, A., Falge, E., Noormets, A., Papale, D., Reichstein, M., and Stauch, V. J.: Cross site evaluation of eddy covariance GPP and RE decomposition techniques, *Agr. Forest Meteorol.*, 148, 821–838, doi:10.1016/j.agrformet.2007.11.012, 2008.
- 755 Domingues, T. F., Berry, J. A., Martinelli, L. A., Ometto, J. and Ehleringer, J. R.: Parameterization of canopy structure and leaf-level gas exchange for an eastern Amazonian tropical rain forest (Tapajós National Forest, Para, Brazil), *Earth Interact.*, 9(17), EI149, doi:10.1175/EI149.1. 2005.
- 760 Domingues, T. F., Martinelli, L. A., and Ehleringer, J. R.: Ecophysiological traits of plant functional groups in forest and pasture ecosystems from eastern Amazonia, Brazil, *Plant Ecol.*, 193, 101–112, 2007
- Eltahir, E. and Bras, R. L.: Precipitation recycling in the Amazon Basin, *Q. J. Roy. Meteor. Soc.*, 120, 861–880, 1994.
- 765 Espírito-Santo, F. D. B., Gloor, M., Keller, M., Malhi, Y., Saatchi, S., Nelson, B., Junior, R. C. O., Pereira, C., Lloyd, J., Frohking, S., Palace, M., Shimabukuro, Y. E., Duarte, V., Mendoza, A. M., López-González, G., Baker, T. R., Feldpausch, T. R., Brienen, J. W., Asner, P., Boyd, D. S. et Phillips, O. L.: Size and frequency of natural forest disturbances and the Amazon forest carbon balance., *Nature communications*, vol. 5, doi : 10.1038/ncomms4434, p. 3434, 2014.
- 770 Farquhar, G. D., von Caemmerer, S., and Berry, J. A.: A biochemical model of photosynthetic CO₂ assimilation in leaves of C3 species, *Planta*, 149, 78–90, 1980.
- 775 Field, C. B. and Mooney, H. A.: The photosynthesis-nitrogen relationship in wild plants, in: *The Economy of Plant Form and Function* (T. J. Givnish, ed.), Cambridge University Press, Cambridge, 25–55, 1986.
- 780 Fisher, R. A., Williams, M., da Costa, A. L., Malhi, Y., da Costa, R. F., Almeida, S., and Meir, P.: The response of an Eastern Amazonian rain forest to drought stress: results and modelling analyses from a throughfall exclusion experiment, *Glob. Change Biol.*, 13, 2361–2378, 2007.
- 785 Foley, J. A., Prentice, C., Ramankutty, N., Levis, S., Pollard, D., Sitch, S. and Haxeltine, A.: An integrated biosphere model of land surface processes, terrestrial carbon balance, and vegetation dynamics, *Global Biogeochem. Cycles*, 10(4), 603–628, doi:10.1029/96GB02692.1996.
- 790 Foley, J. A., Costa, M. H., Delire, C., Ramankutty, N. and Snyder, P. : Green surprise? How terrestrial ecosystems could affect earth's climate. *Frontiers in Ecology and the Environment*, 1(1), 38-44. 2003.
- Friedlingstein, P., Cox, P., Betts, R., Bopp, L., von Bloh, W., Brovkin, V., Cadule, P., Doney, S., Eby, M., Fung, I., Bala, G., John, J., Jones, C., Joos, F., Kato, T., Kawamiya, M., Knorr, W., Lindsay, K., Matthews, H. D., Raddatz, T., Rayner, P., Reick, C., Roeckner, E., Schnitzler, K. G., Schnur, R., Strassmann, K., Weaver, A. J., Yoshikawa, C., and Zeng, N.: Climatecarbon cycle feedback analysis: results from the C4MIP model inter- comparison, *J. Climate*, 19, 3337–3353, 2006.
- 795 Fu, R., Yin, L., Li, W., Arias, P. A., Dickinson, R. E., Huang, L., Chakraborty, S., Fernandes, K., Liebmann, B., Fisher, R. A., and Myneni, R. B.: Increased dry-season length over southern Amazonia in recent decades and its implication for future climate projection, *P. Natl. Acad. Sci. USA*, 110, 18110–18115, doi:10.1073/pnas.1302584110, 2013.
- 800 Gatti, L. V., Miller, J. B., D'Amelio, M. T. S., Martinewski, A., Basso, L. S., Gloor, M. E., Wofsy,

- S., and Tans, P.: Vertical profiler of CO₂ above eastern Amazonia suggest a net carbon flux to the atmosphere and balanced biosphere between 2000 and 2009, *Tellus B*, 581–594, 20, doi:10.1111/j.1600-0889.2010.00484.x, 2010.
- 805 Gatti, L. V., Gloor, M., Miller, J. B., Doughty, C. E., Malhi, Y., Domingues, L. G., Basso, L. S., Martinewski, A., Correia, C. S. C., and Borges, V. F.: Drought sensitivity of Amazonian carbon balance revealed by atmospheric measurements, *Nature*, 506, 76–80, 2014.
- 810 Gloor, M., Gatti, L., Brienen, R., Feldpausch, TR, Phillips, OL, Miller, J, Ometto, JP, Rocha, H, Baker, T, De Jong, B, Houghton, RA, Malhi, Y, C Aragão, LEO, Guyot, J-L, Zhao, K, Jackson, R, Peylin, P, Sitch, S, Poulter, B, Lomas, M, Zaehle, S, Huntingford, C, Levy, P and Lloyd, J: The carbon balance of South America: A review of the status, decadal trends and main determinants. *Biogeosciences*, 9 (12). 5407 - 5430 . 2012.
- 815 Good, P., Jones, C., Lowe, J., Betts, R., and Gedney, N.: Comparing tropical forest projections from two generations of Hadley Centre Earth System models, HadGEM2-ES and HadCM3LC, *J. Climate*, 26, 495–511, 2013.
- 820 Goudriaan, J., H.H. van Laar, H. van Keulen & W. Louwse: Photosynthesis, CO₂ and plant production. In: W. Day & R.K. Atkin (Eds.), *Wheat growth and modelling*. NATO AS/ Series, Series A, Vol 86. Plenum Press, New York, 107-122. 1985
- 825 Goudriaan, J., 1986: A simple and fast numerical method for the computation of daily totals of crop photosynthesis. *Agric. For. Meteorol.*, 38, 249-254.1986.
- Grant, R., Hutrya, L., and Oliveira, R.: Modeling the carbon balance of Amazonian rain forests : resolving ecological controls on net ecosystem productivity, *Ecological monographs*, 79,3, 445–463, 2009.
- 830 Gibelin, A. L., Calvet, J. C., and Viovy, N.: Modelling energy and CO₂ fluxes with an interactive vegetation, land surface model, Evaluation at high and middle latitudes, *Agr. Forest Meteorol.*, 148, 1611–1628, 2008.
- 835 Hollinger, D.Y., Richardson, A.D.: Uncertainty in eddy covariance measurements and its application to physiological models. *Tree Physiol.* 25, 873–885.2005.
- 840 Huntingford, C., Zelazowski, P., Galbraith, D., Mercado, L. M., Sitch, S., Fisher, R. A., Lomas, M., Walker, A. P., Jones, C. D., Booth, B. B. B., Malhi, Y., Hemming, D., Kay, G., Good, P., Lewis, S. L., Phillips, O. L., Atkin, O. K., Lloyd, J., Gloor, E., Zaragoza-Castells, J., Meir, P., Betts, R., Harris, P. P, Nobre, C., Marengo, C., and Cox, P. M.: Simulated resilience of tropical rainforests to CO₂-induced climate change, *Nat. Geosci.*, 6, 268– 273, 2013.
- 845 Jackson, R. B., J. Canadell, J. R. Ehleringer, H. A. Mooney, O. E. Sala, and Schulze, E. D. : A global analysis of root distributions for terrestrial biomes, *Oecologia*, 108 , 389–411. 1996.
- Jacobs, C. M. J.: Direct impact of atmospheric CO₂ enrichment on regional transpiration, Ph.D. thesis, Agricultural University, Wageningen, 1994.
- 850 Joetzjer, E., Douville, H., Delire, C., and Ciais, P.: Present-day and future Amazonian precipitation in global climate models: CMIP5 versus CMIP3, *Clim. Dynam.*, 41, 2921–2936, 2013.
- Joetzjer, E., Delire, C., Douville, H., Ciais, P., Decharme, B., Fisher, R., Christoffersen, B., Calvet, J. C., da Costa, A. C. L., Ferreira, L. V. and Meir, P.: Predicting the response of the Amazon rainforest to persistent drought conditions under current and future climates: a major challenge for global land

- 855 surface models. *Geoscientific Model Development*, 7, 2933–2950, doi:10.5194/gmd-7-2933-2014, 2014
- Jones, C., Robertson, E., Arora, V., Friedlingstein, P., Shevliakova, E., Bopp, L., V. Brovkin, T. Hajima, E. Kato, Kawamiya, M., Liddicoat, S., Lindsay, K., Reick, C. H, Roelandt, C., Segschneider, J. et Tjiputra, J. :Twenty-first-century compatible CO₂ emissions and airborne fraction simulated by CMIP5 Earth System Models under four representative concentration pathways. *Journal of Climate*, 26(13), 4398-4413, 2013.
- 860
- Keenan, T. F., Hollinger, D. Y., Bohrer, G., Dragoni, D., Munger, J. W., Schmid, H. P., and Richardson, A. D.: Increase in forest water-use efficiency as atmospheric carbon dioxide concentrations rise, *Nature*, 499, 324–327, doi:10.1038/nature12291, 2013.
- 865
- Kim, Y., Knox, R. G., Longo, M., Medvigy, D., Hutyra, L. R., Pyle, E. H., Wofsky, S. C., Bras, R. L. and Moorcroft, P. R. : Seasonal carbon dynamics and water fluxes in an Amazon rainforest. *Global Change Biology*, 18(4), 1322-1334. 2012.
- 870
- Krinner, G., Viovy, N., de Noblet-Ducoudre, N., Ogee, J., Polcher, J., Friedlingstein, P., Ciais, P., Sitch, S., and Prentice, I.: A dynamic global vegetation model for studies of the coupled atmosphere-biosphere system, *Global Biogeochem. Cy.*, 19, 1–33, 2005.
- 875
- Kucharik, C.J., Foley, J.A., Delire, C., Fisher, V.A., Coe, M.T., Lenters, J.D., Young-Molling, C., Ramankutty, N., Norman, J.M., Gower, S.T.: Testing the performance of a dynamic global ecosystem model: water balance, carbon balance, and vegetation structure. *Global Biogeochem. Cycles* 14, 795–825. 2000.
- 880
- Kruijt, B., Elbers, J.A., von Randow, C., Araújo, A.C., Oliveira, P.J., Culf, A., Manzi, A.O., Nobre, A.D., Kabat, P., Moors, E.J.: The robustness of eddy correlation fluxes for Amazon rain forest conditions. *Ecol. Appl.* 14, 101–113. 2004.
- 885
- Lemaire and Gastal: N Uptake and Distribution in Plant Canopies. In G. Lemaire (eds.) *Diagnosis of the Nitrogen Status in Crops*, Springer-Verlag, Heidelberg, 3-43, doi 10.1007/978-3-642-60684-7_1, 1997.
- Lewis, S. L., Lloyd, J., Sitch, S., Mitchard, E. T. and Laurance, W. F.: Changing ecology of tropical forests: evidence and drivers. *Annual Review of Ecology, Evolution, and Systematics*, 40, 529-549. 2009.
- 890
- Lloyd, J., and J.A. Taylor, On the temperature dependence of soil respiration, *Functional Eco*, 8, 315-323, 1994.
- 895
- Malhi, Y., Wood, D., Baker, T. R., Wright, J., Phillips, O. L., Cochrane, T., Meir, P., Chave, J., Almeida, S., Arroyo, L., Higuchi, N., Killeen, T. J., Laurance, S. G., Laurance, W. F., Lewis, S. L., Monteagudo, A., Neill, D. A., NúñezVargas, P., Pitman, N. C. A., Quesada, C. A., Salomão, R., Silva, J. N. M., Torres Lezama, A., Terborgh, J., Vásquez Martínez, R., and Vinceti, B.: The regional variation of aboveground live biomass in old growth Amazonian forests, *Glob. Change Biol.*, 12, 1107–1138, 2006
- 900
- Malhi, Y., Aragao, L. E. O., Metcalfe, D. B., Paiva, R., Quesada, C. A., Almeida, S., Anderson, L., Brando, P., Chamber, J. Q., and da Costa, A. C. L.: Comprehensive assessment of carbon productivity, allocation and storage in three Amazonian forests, *Glob. Change Biol.*, 15, 1255–1274, 2009.
- 905
- Malhi, Y., Doughty, C., and Galbraith, D.: The allocation of ecosystem net primary productivity in tropical forests, *Philos. T. R. Soc. B*, 366, 3225–3245, 2011.

- 910 Marengo, J. A., Tomasella, J., Alves, L. M., Soares, W. R., & Rodriguez, D. A.: The drought of 2010 in the context of historical droughts in the Amazon region. *Geophysical Research Letters*, 38(12), 2011.
- Meir, P., Grace, J., and Miranda, A. C.: Leaf respiration in two tropical rainforests: constraints on physiology by phosphorus, nitrogen and temperature, *Funct. Ecol.*, 15, 378–387, 2001.
- 915 Meir, P., Metcalfe, D. B., Costa, A. C. L., and Fisher, R. A.: The fate of assimilated carbon during drought: impacts on respiration in Amazon rainforests, *Philos. T. Roy. Soc. B*, 363, 1849–1855, doi:10.1098/rstb.2007.0021, 2008.
- 920 Mercado, L. M., J. Lloyd, A. J. Dolman, S. Sitch, and S. Patiño: Modelling basin-wide variations in Amazon forest productivity Part 1: Model calibration, evaluation and upscaling functions for canopy photosynthesis, *Biogeosciences*, 6, 1247–1272, doi:10.5194/bg-6-1247-2009. 2009.
- 925 Metcalfe, D. B., Meir, P., Aragao, L. E. O. C., Lobo-do-Vale, R., Galbraith, D., Fisher, R. A., Chaves, M. M., Maroco, J. P., da Costa, A. C. L., de Almeida, S. S., Braga, A. P., Gonçalves, P. H. L., de Athaydes, J., da Costa, M., Portela, T. T. B., de Oliveira, A. A. R., Malhi, and Williams, M.: Shifts in plant respiration and carbon use efficiency at a large-scale drought experiment in the eastern Amazon, *New Phytol.*, 187, 608–621, 2010.
- 930 Nachtergaele, F., van Velthuizen, H., Verelst, L., and Wiberg, D.: Harmonized World Soil Database, Version 1.2, FAO, IIASA, ISRIC, ISSCAS, JRC, available at: <http://www.iiasa.ac.at/Research/LUC/External-World-soil-database/HTML/> (last access: 15 November 2012), 2012.
- 935 Noilhan, J. and Planton, S.: A simple parameterization of land surface processes for meteorological models, *Mon. Weather Rev.*, 117, 536–549, 1989.
- Noilhan, J. and Mahfouf, J.-F.: The ISBA land surface parameterisation scheme, *Glob. Planet Chang.*, 13, 145–159, 1996.
- 940 Pan, Y., Birdsey, R. A., Fang, J., Houghton, R., Kauppi, P. E., Kurz, W. A., Phillips, O. L., Shvidenko, A., Lewis, S. L., Canadell, J. G., Ciais, P., Jackson, R. B., Pacala, S.W., McGuire, A. D., Piao, S., Rautiainen, A., Sitch, S., and Hayes, D.: A large and persistent carbon sink in the world's forests, *Science*, 333, 988–993, 2011.
- 945 Parton, W., Stewart, J., Cole, C.: Dynamics of C, N, P and S in grassland soils: a model. *Biogeochemistry* 5 (1), 109–131, 1988.
- Phillips, O. L., Lewis, S. L., Baker, T. R., Chao, K. J. and Higuchi, N.: The changing Amazon forest. *Philosophical Transactions of the Royal Society B: Biological Sciences*, 363(1498), 1819–1827, 2008.
- 950 Potter, C. S. and Klooster, S. A.: Detecting a terrestrial biosphere sink for carbon dioxide: interannual ecosystem modeling for the mid 1980s, *Clim. Change*, 42, 489–503, 1999.
- 955 Pyle, E. H., Santoni, G. W., Nascimento, H. E. M., Hutyrá, L. R., Vieira, S., Curran, D. J., van Haren, J., Saleska, S. R., Chow, V. Y., Carmago, P. B., Laurance, W. F., and Wofsy, S. C.: Dynamics of carbon, biomass, and structure in two amazonian forests, *J. Geophys. Res. Biogeosci.*, 113, G00b08, doi:10.1029/2007jg000592, 2008
- 960 Randerson, J. T., Hoffman, F. M., Thornton, P. E., Mahowald, N. M., Lindsay, K., Lee, Y.-H., Nevison, C. D., Doney, S. C., Bonan, G., Stoeckli, R., Covey, C., Running, S.W., and Fung, I.Y.: Systematic assessment of terrestrial biogeochemistry in coupled climate-carbon models, *Glob. Change Biol.*, 15, 2462–2484, 2009.

- 965 Reich, P. B., Tjoelker, M. G., Machado, J. L. and Oleksyn, J.: Universal scaling of respiratory metabolism, size and nitrogen in plants. *Nature*, 439, 457–461. 2006.
- Reichstein, M., Falge, E., Baldocchi, D., Papale, D., Aubinet, M., Berbigier, P., Bernhofer, C., Buchmann, N., Gilmanov, T., Granier, A., Grunwald, T., Havrankova, K., Ilvesniemi, H., Janous, D.,
970 Knohl, A., Laurila, T., Lohila, A., Loustau, D., Matteucci, G., Meyers, T., Miglietta, F., Ourcival, J. M., Pumpanen, J., Rambal, S., Rotenberg, E., Sanz, M., Tenhunen, J., Seufert, G., Vaccari, F., Vesala, T., Yakir, D., and Valentini, R.: On the separation of net ecosystem exchange into assimilation and ecosystem respiration: Review and improved algorithm, *Glob. Change Biol.* 11, 1424–1439, doi:10.1111/j.1365-2486.2005.001002.x, 2005.
- 975 Rice, A. H., Pyle, E. H., Saleska, S. R., Hutyyra, L., Palace, M., Keller, M., de Camargo, P. B., Portilho, K., Marques, D. F., and Wofsy, S. C.: Carbon balance and vegetation dynamics in an old-growth amazonian forest, *Ecol. Appl.*, 14, 55–71, doi:10.1890/02-6006, 2004.
- 980 da Rocha, H. R., Goulden, M. L., Miller, S. D., Menton, M. C., Pinto, L. D., de Freitas, H. C. and Silva Figueira, A.M.: Seasonality of water and heat fluxes over a tropical forest in eastern Amazonia. *Ecological Applications* 14, S22–S32. 2004.
- da Rocha, H. R., Manzi, A. O., Cabral, O. M., Miller, S. D., Goulden, M. L., Saleska, S. R., Restro-
985 Coupe, N., Wofsy, S. C., Borma, L. S., Artaxo, P., Vourlitis, G., Nogueira, J. S., Cardoso, F. L., Nobre, A. D., Kruijt, B., Freitas, H. C., von Randow, C., Aguiar, R. G., and Maia, J. F.: Patterns of water and heat flux across a biome gradient from tropical forest to savanna in Brazil, *J. Geophys. Res. Biogeo.*, 114, G00B12, doi:10.1029/2007JG000640, 2009.
- 990 de Rosnay, P., Bruen, M., and Polcher, J.: Sensitivity of surface fluxes to the number of layers in the soil model used in GCMs, *Geophys. Res. Lett.*, 27, 3329–3332, doi:10.1029/2000GL011574, 2000.
- de Rosnay, P., Polcher, J., Bruen, M., and Laval, K.: Impact of a physically based soil water flow and
995 soil-plant interaction representation for modeling large-scale land surface processes, *J. Geophys. Res.-Atmos.*, 107, 4118, doi:10.1029/2001JD000634, 2002.
- Rowland, L., Hill, T. C., Stahl, C., Siebicke, L., Burban, B., Zaragoza-Castells, J., Ponton, S., Bonal, D., Meir, P. and Williams, M.: Evidence for strong seasonality in the carbon storage and carbon use efficiency of an Amazonian forest, *Global change biology*, 20,3, doi :10.1111/gcb.12375, p. 979–91,
1000 ISSN 1365-2486, 2014
- Ruimy, A., Dedieu, G., and Saugier, B.: Turc: A diagnostic model of continental gross primary productivity and net primary productivity, *Global Biogeochem. Cy.*, 10, 269–285, doi:10.1029/96gb00349, 1996.
1005
- Saleska, S. R., Miller, S. D., Matross, D. M., Goulden, M. L., Wofsy, S. C., da Rocha, H. R., de Camargo, P. B., Crill, P., Daube, B. C., de Freitas, H. C., Hutyyra, L., Keller, M., Kirchhoff, V., Menton, M., Munger, J. W., Pyle, E. H., Rice, A. H., and Silva, H.: Carbon in amazon forests: Unexpected seasonal fluxes and disturbance-induced losses, *Science*, 302, 1554–1557, 2003.
1010
- Shuttleworth J. W., Gash J. H. C., Lloyd C. R. Moore, C. J., Roberts, J., Marques, A. D., Fisch, G., Silva, V. D., Ribeiro, M. D. G., Molion, L. C. B., Sa, L. D. D., Nobre, J. C. A., Cabral, O. M. R., Patel, S. R. And Demoraes J. C.: Eddy correlation measurements of energy partition for Amazonian forest. *Quarterly Journal of the Royal Meteorological Society*, 110, 1143–1162. 1984.
1015
- Taylor, K. E. Summarizing multiple aspects of model performance in a single diagram, *J. Geophys. Res.*, 106, 7183–7192, doi:10.1029/2000JD900719, 2001.

- 1020 Sitch, S., Smith, B., Prentice, I. C., Arneth, A., Bondeau, A., Cramer, W., Kaplan, J.O., Levis, S., Lucht, W., and Sykes, M. T.: Evaluation of ecosystem dynamics, plant geography and terrestrial carbon cycling in the LPJ dynamic global vegetation model, *Glob. Change Biol.*, 9, 161–185, 2003.
- 1025 Valentini, R., Matteucci, G., Dolman, A. J., Schulze, E. D., Rebmann, C., Moors, E. J., Granier, A., Gross, P., Jensen, N. O., and Pilegaard, K.: Respiration as the main determinant of carbon balance in European forests, *Nature*, 404, 861–865, 2000.
- Van Heemst : Potential crop production, in *Modelling of Agricultural Production: Weather, Soil and Crops. Simulation Monographs*, edited by H. Van Keulen and J. Wolf, Pudoc, Wageningen.1986.
- 1030 Verbeeck, H., Peylin, P., Bacour, C., Bonal, D., Steppe, K., and Ciais, P.: Seasonal patterns of CO₂ fluxes in Amazon forests: Fusion of eddy covariance data and the ORCHIDEE model, *J. Geo phys. Res. Biogeo.*, 116, G02018, doi:10.1029/2010JG001544, 2011.
- 1035 De Weirdt, M., Verbeeck, H., Maignan, F., Peylin, P., Poulter, B., Bonal, D., Ciais, P., and Steppe, K.: Seasonal leaf dynamics for tropical evergreen forests in a process-based global ecosystem model, *Geosci. Model Dev.*, 5, 1091–1108, doi:10.5194/gmd-5- 1091-2012, 2012.

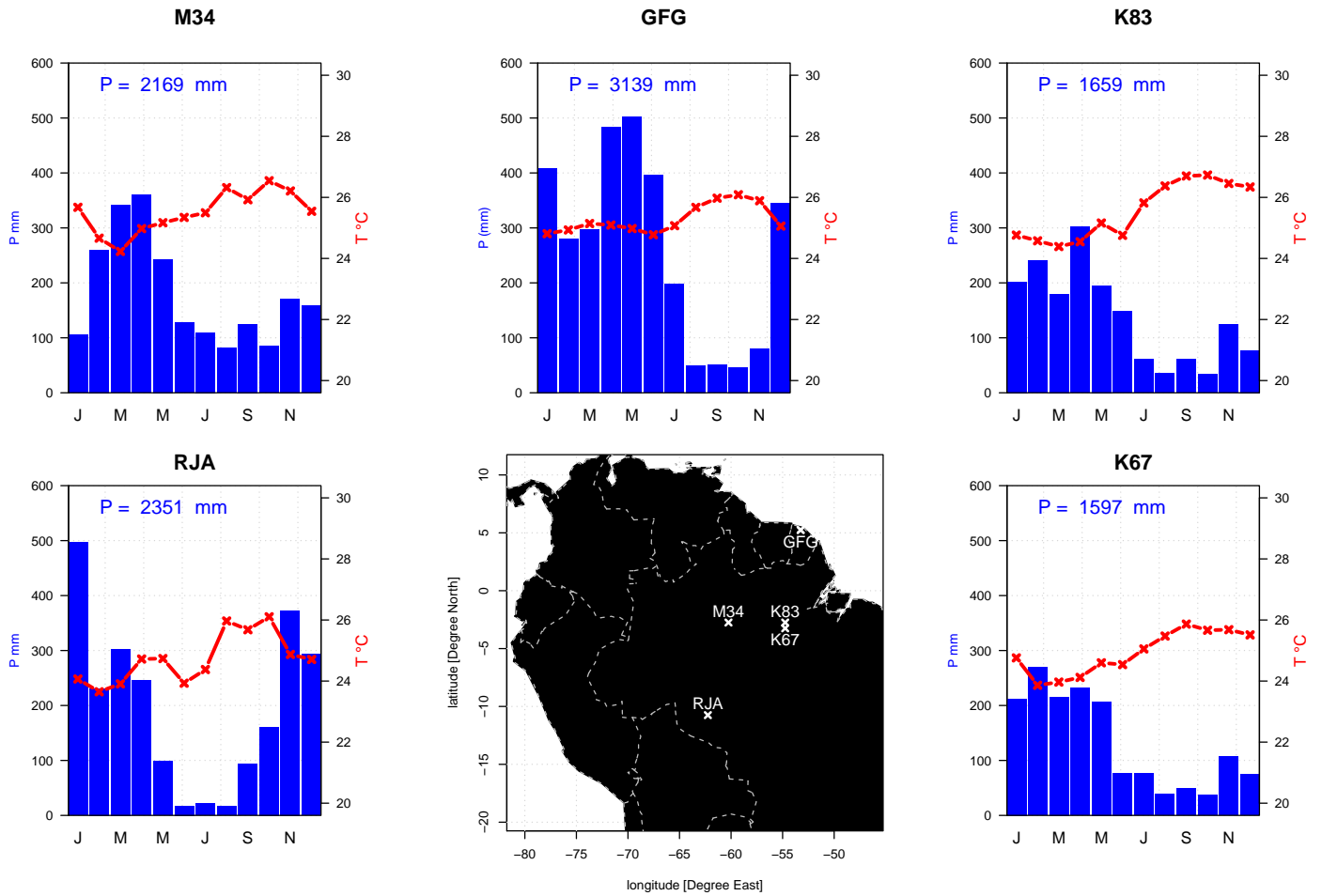


FIGURE 1 – Mean annual cycle of precipitation (blue), temperature (red) calculated over 3 years (see table 1) and location of the fluxtowers used in this study.

TABLE 1 – Characteristics and references of fluxtowers used in this study.

Site	CODE	Cover Period	Texture (fraction)	Root depth	Soil depth	References
Manaus km34	M34	2003 → 2005	CLAY=0.68; SAND=0.20	8m	12m	Araujo et al. (2002)
Paracou	GFG	2007 → 2009	CLAY=0.51; SAND=0.33	8m	12m	Bonal et al. (2008)
Santarem km83	K83	2001 → 2003	CLAY=0.80; SAND=0.18	8m	12m	Goulden et al. (2004)
Santarem km67	K67	2002 → 2004	CLAY=0.42; SAND=0.52	8m	12m	Saleska et al. (2003)
Reserva Jarù	JRU	2000 → 2003	CLAY=0.10; SAND=0.80	4m	4m	Kruijt et al. (2004)

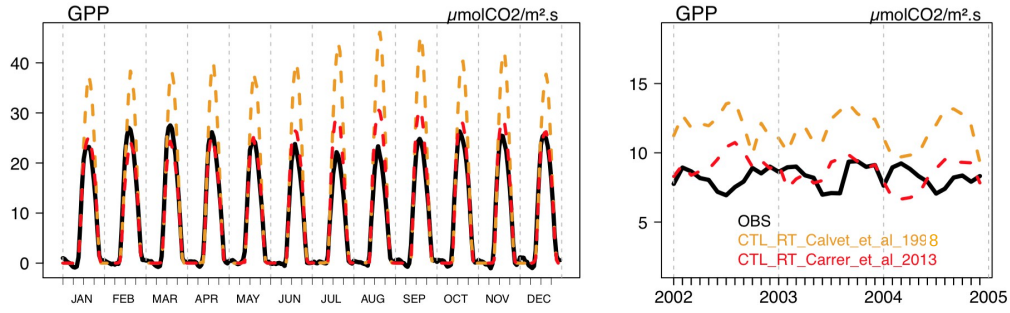


FIGURE 2 – Observed and simulated GPP with the CTL version of $ISBA_{CC}$ comparing the two radiative transfers at K67. Left panel shows the diurnal cycle for each month averaged over 3 years (2002–2004); right panel, monthly mean time series for 2001–2003.

TABLE 2 – $ISBA_{CC}$: Nomenclature

Symbols	Units	Description
A_m	$kg_{CO_2} m^{-2} s^{-1}$	Photosynthesis rate (light saturated)
C_a	ppmv	Atmospheric CO_2 concentration
C_i	ppmv	Leaf internal CO_2 concentration
D_s	$g kg^{-1}$	Saturation deficit at the leaf surface
D_{max}	$g kg^{-1}$	Maximum value of D_s
f	unitless	coupling factor
f_0	unitless	coupling factor at saturating air humidity ($D_s = 0$)
f_0^*	unitless	coupling factor in well-watered conditions and at saturating air humidity ($D_s = 0$)
f_{min}	unitless	coupling factor at maximum air humidity deficit ($D_s = D_{max}$)
Γ	ppmv	CO_2 concentration compensation point
g_m	$mm s^{-1}$	Mesophyll conductance defined as the light saturated rate of photosynthesis (Jacobs 1994)
g_m^*	$mm s^{-1}$	g_m in well-watered conditions
g_s	$mm s^{-1}$	Stomatal conductance

TABLE 3 – *ISBA_{CC}* Modifications : **Photosynthesis & Transpiration PS** version

Parameter	CTL	PS	
$A_{m,max}$	$2.2 \cdot 10^{-6}$	$0.36 \cdot 10^{-6}$	
g_m	$g_m = g_m^*$ $g_m = g_m^* - (g_m^* - g_m^N) \cdot \frac{(1 - SWI)}{(1 - SWI_c)}$ $g_m = g_m^N \cdot \frac{SWI}{SWI_c}$	$g_m = g_m^*$ $g_m = SWI \cdot g_m^*$ $g_m = SWI \cdot g_m^*$	$SWI \geq 1$ $SWI_c < SWI < 1$ $SWI \leq SWI_c$
f_0	$f_0 = \frac{4.7 - \ln(g_m)}{7}$ $f_0 = \frac{2.8 - \ln(g_m)}{7}$	$f_0 = 0.74$ $f_0 = 0.74$	$SWI_c < SWI$ $SWI \leq SWI_c$
Symbol used			
$A_{m,max}$ ($kg_{CO_2} m^{-2} s^{-1}$)	maximum photosynthesis rate for C_3 plants		
SWI	Soil Wetness index $\left(SWI = \frac{\Theta - \Theta_{wilt}}{\Theta_{fc} - \Theta_{wilt}} \right)$		
Θ	Soil water content ($m^3 m^{-3}$)		
Θ_{fc}	Field capacity ($m^3 m^{-3}$)		
Θ_{wilt}	Wilting point ($m^3 m^{-3}$)		
SWI_c	Critical extractable Soil Wetness Index ($SWI_c = 0.3$)		
g_m^N	Value of g_m at $SWI = SWI_c$ in $mm s^{-1}$		
g_m^* ($mm s^{-1}$)	Value of g_m in well-watered conditions ($SWI \geq 1$). ($g_m = 2 mm s^{-1}$ for broadleaf tropical forest)		

TABLE 4 – *ISBA_{CC}* : Modifications **autotrophic respiration functions PS+R** version

Parameter	CTL	PS+R
$\frac{1}{SLA}$	$\simeq 68.5 \text{ gDM m}^{-2}$	$= 120 \text{ gDM m}^{-2}$
R_{leaves}	$\frac{A_m}{9}$	$\frac{A_m}{9} \cdot \exp(-k_n \cdot LAI) \cdot \frac{1}{LAI}; k_n = 0.2$
R_2	$B_2 \cdot \eta \cdot Q_{10}^{\frac{T_s-25}{10}}; \eta = 0.01 \text{ g/g day}^{-1}$ and $Q_{10} = 2$	$B_2 \cdot \beta \cdot f(T_s); \beta = 1.25$
R_4	$B_4 \cdot R_0(1 + 0.16T_p); R_0 = 1.9 \cdot 10^{-4} \text{ g/g day}^{-1}$	$B_4 \cdot \beta \cdot f(T_p); \beta = 1.25$
R_5	0	$B_5 \cdot \lambda_{sap} \beta_{wood} \cdot f(T_s); \beta_{wood} = 0.0125$
		$f(T) = \exp \left\{ E_0 \left(\frac{1}{15 - T_0} - \frac{1}{T - T_0} \right) \right\};$ $T_0 = 25^{\circ}C$
Symbol used		
T_s	surface temperature	
T_p	soil temperature	
λ_{sap}	fraction of sap wood	

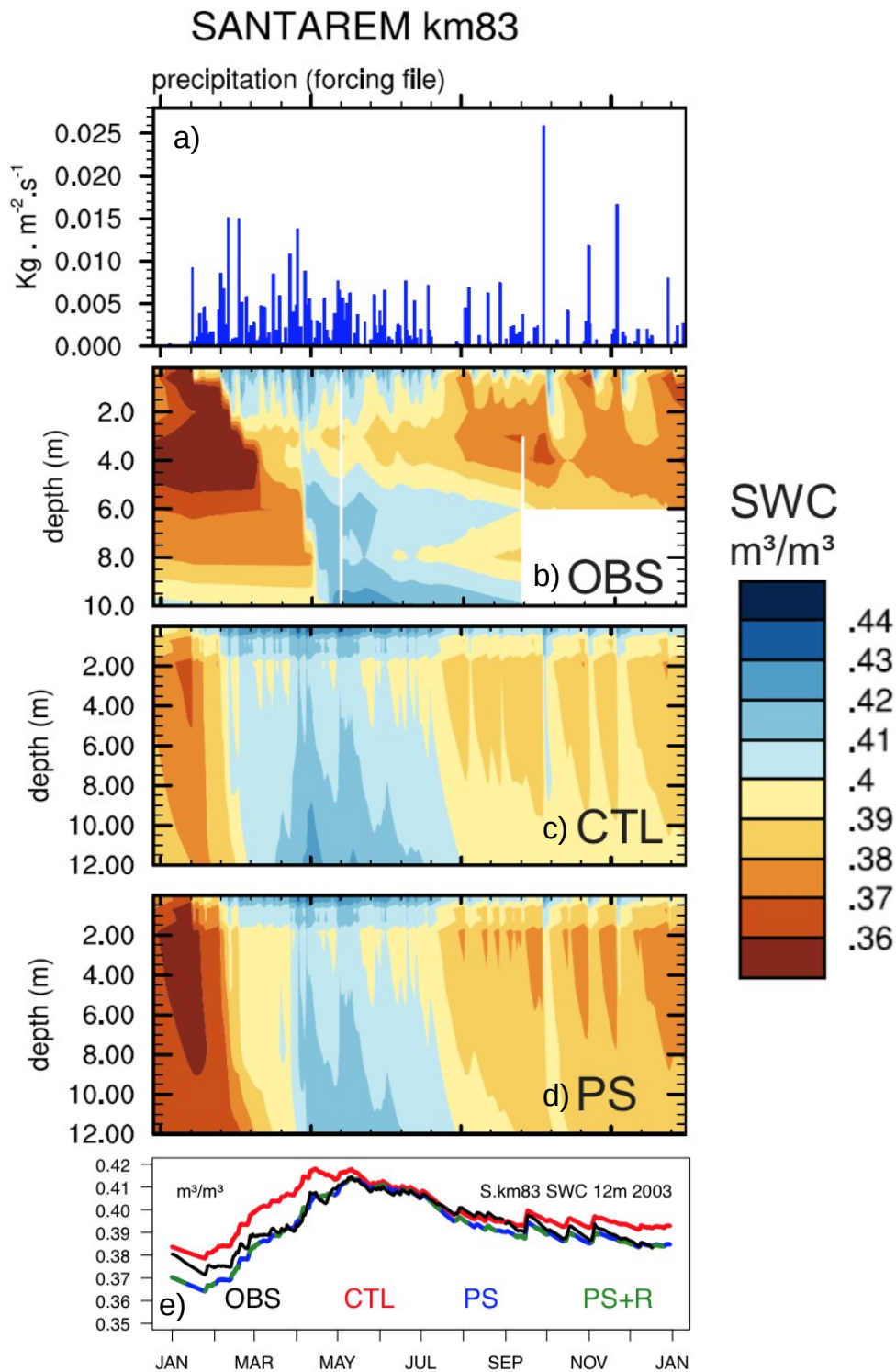


FIGURE 3 – Daily precipitation (a), observed (b) and simulated (c and d) soil moisture at K83 during 2003. The total soil water content over the whole 12 m column is shown on plot e. We linearly rescaled the soil moisture content of the 10 m pit (Bruno et al., 2006) to the values of the 2 m one (da Rocha et al., 2004) by multiplying the 10m SWC by the ratio of field capacities between the 2m and the 10m pit).

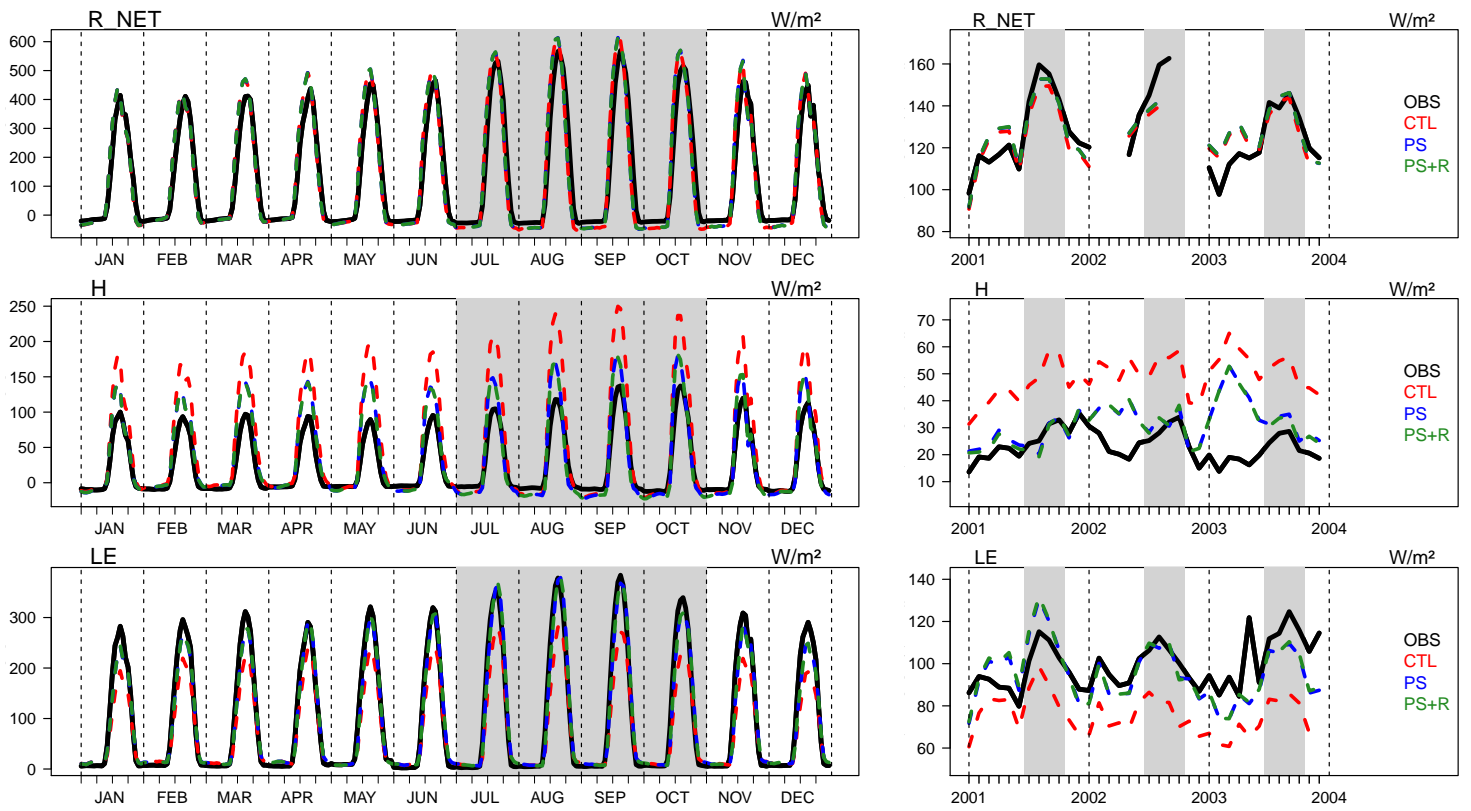


FIGURE 4 – Observed and simulated net radiation (R_{Net}), sensible heat (H) and latent heat (LE) at K83. Left panels show the diurnal cycle for each month averaged over 3 years (2001–2003); and right panels, monthly mean time series for 2001–2003. Gray shaded areas indicate dry seasons (defined as periods with precipitation less than $100 \text{ mm month}^{-1}$).

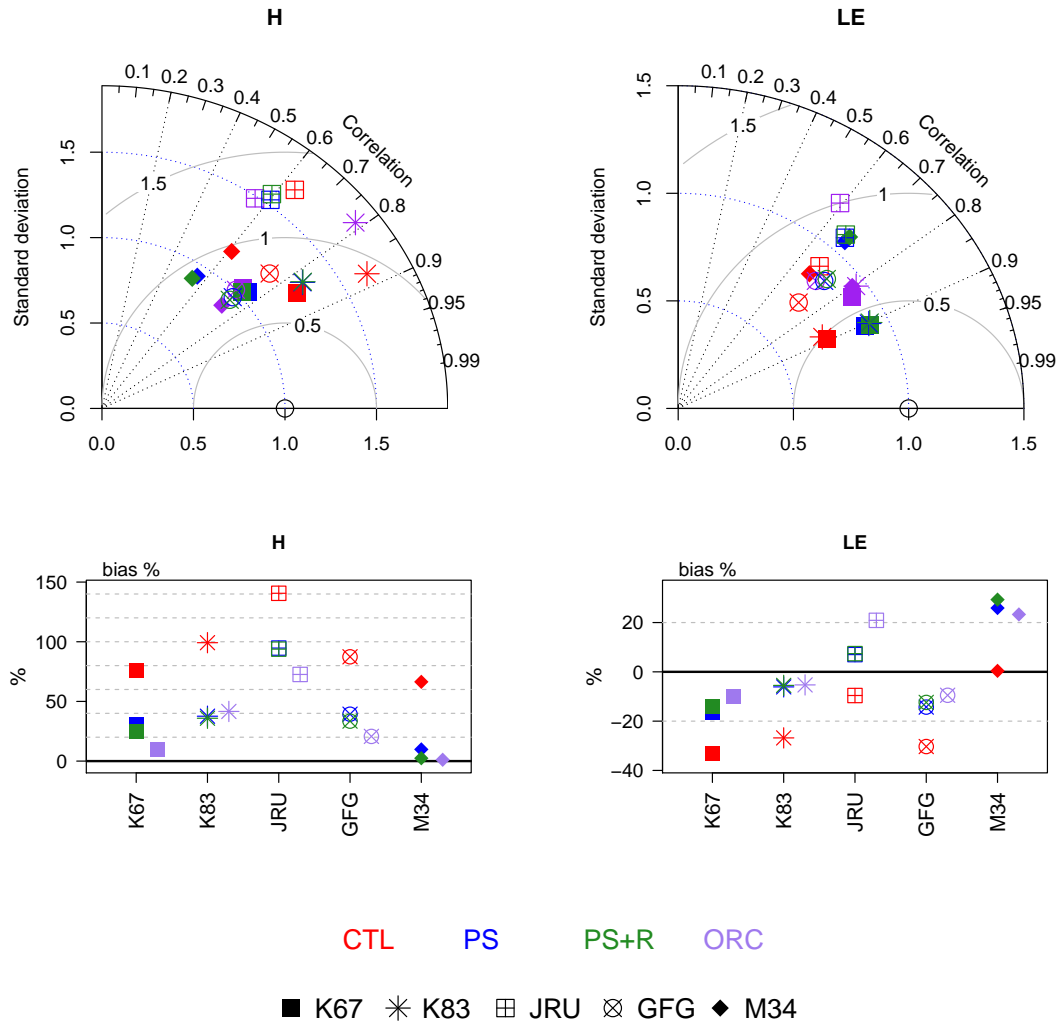


FIGURE 5 – Taylor diagrams (top) and bias (%) (bottom) calculated among hourly values removing night values (Short Wave down $\leq 5 \text{ W m}^{-2}$) for H and LE at the five fluxtowers and for each available period (see table 1). In the Taylor diagrams, correlation extends radially from the origin. The blue lines indicate identical ratios of standard deviation of the simulated flux to the observed flux. The grey lines represent identical root mean square errors (RMSE) of the centered fluxes.

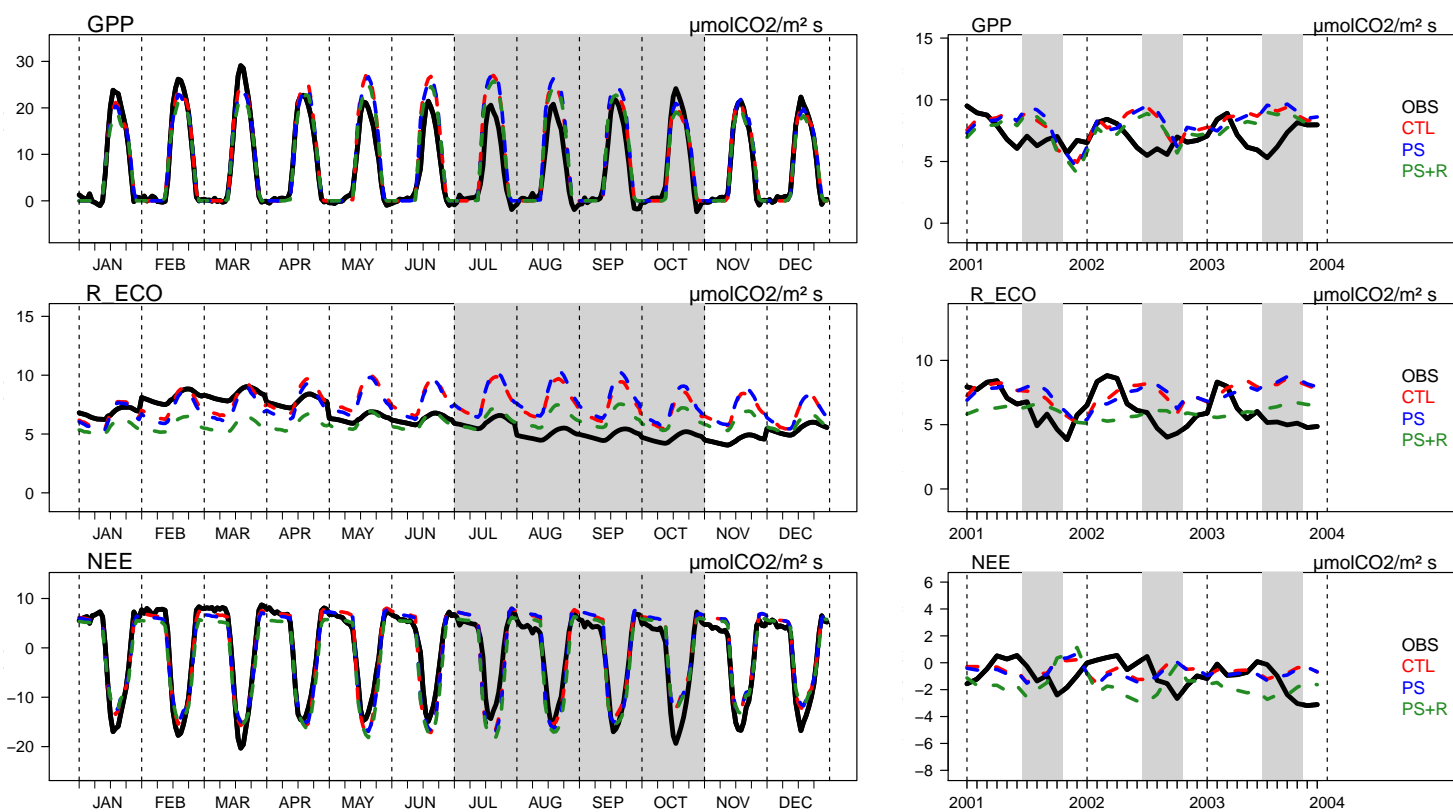


FIGURE 6 – Observed and simulated GPP, R_{ECO} and NEE at k83. Left panels show the diurnal cycle for each month averaged over 3 years (2001–2003); and right panels, monthly mean time series for 2001–2003. Gray shaded areas indicate dry seasons (defined as periods with precipitation less than $100 \text{ mm month}^{-1}$).

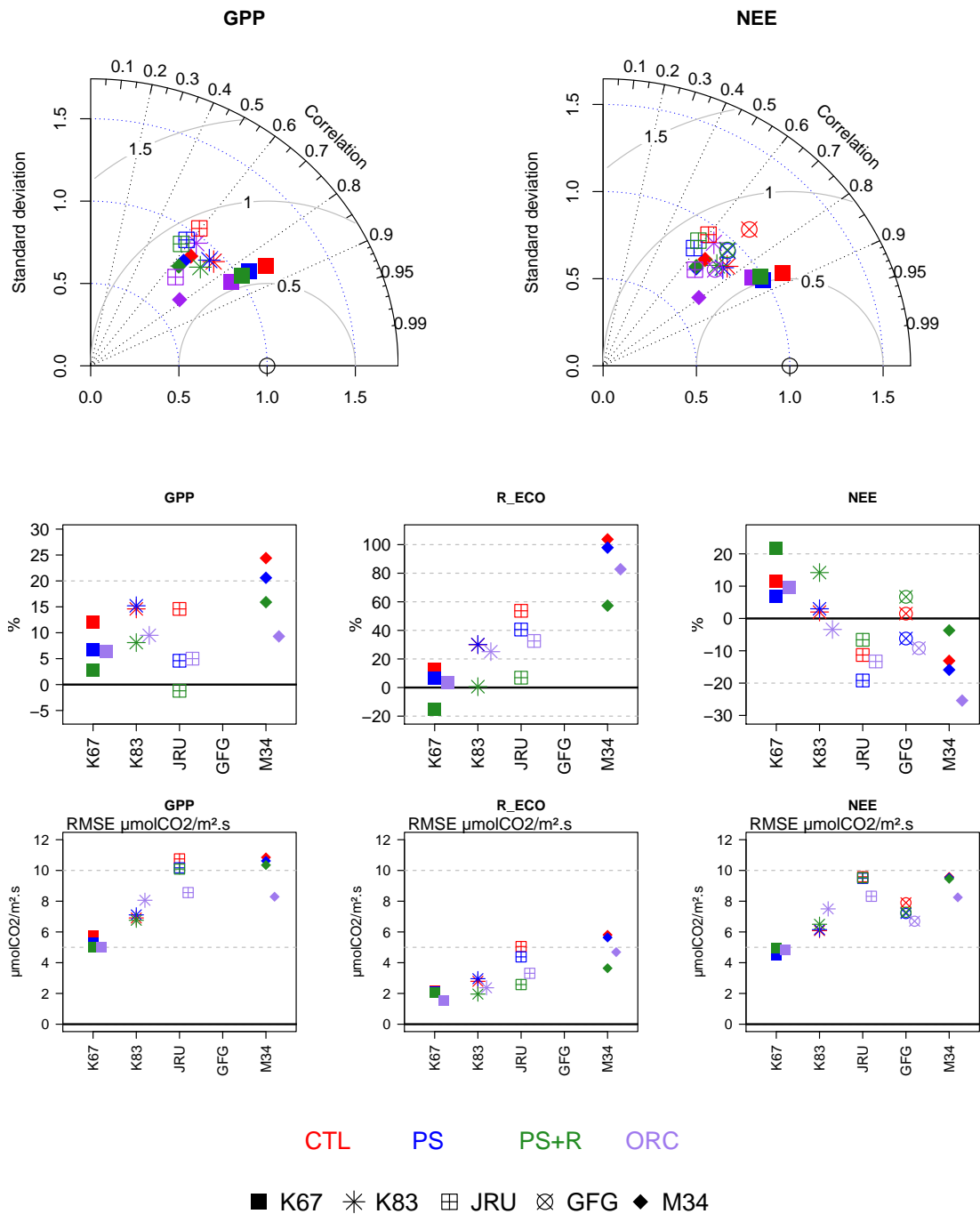


FIGURE 7 – Taylor diagrams (top) for GPP and NEE and bias for GPP R_{ECO} and NEE (%) (bottom) calculated among hourly values removing night values (Short Wave down $\leq 5 \text{ W m}^{-2}$) at the five fluxtowers and for each available period (see table 1). Note that at GFG only NEE timeseries was available. In the Taylor diagrams, correlation extends radially from the origin. The blue lines indicate identical ratios of standard deviation of the simulated flux to the observed flux. The grey lines represent identical root mean square errors (RMSE) of the centered fluxes.

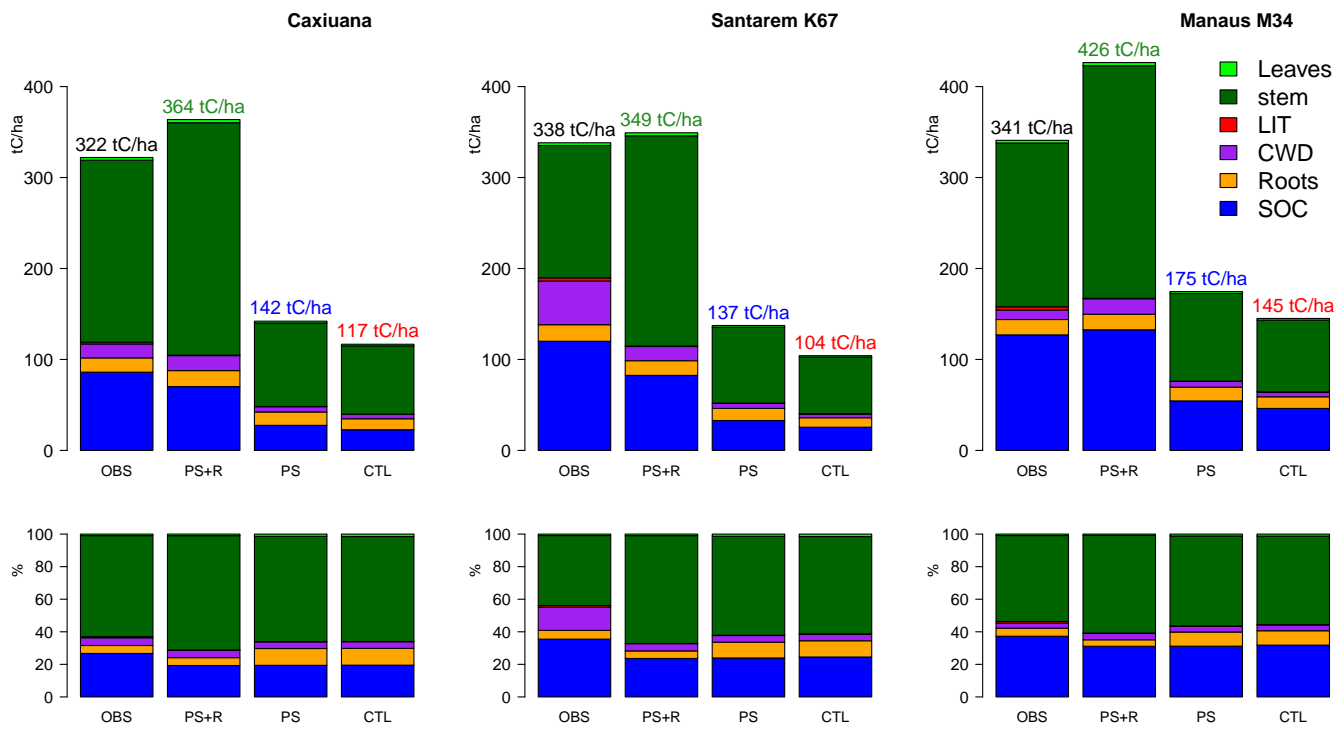


FIGURE 8 – Observed (Mahli et al 2009) and simulated (CTL, PS and PS+R) annual carbon pools (Leaves (B_L), Stem ($B_2 + B_5$), Litter (LIT), Coarse and Woody Debris (CWD), Roots ($B_4 + B_6$) and Soil Organic Content (SOC)) at Caxiuana, K67 and M34. Top panels show the absolute carbon stock in $tC\ ha^{-1}$ and below panels the relative carbon stock (%).

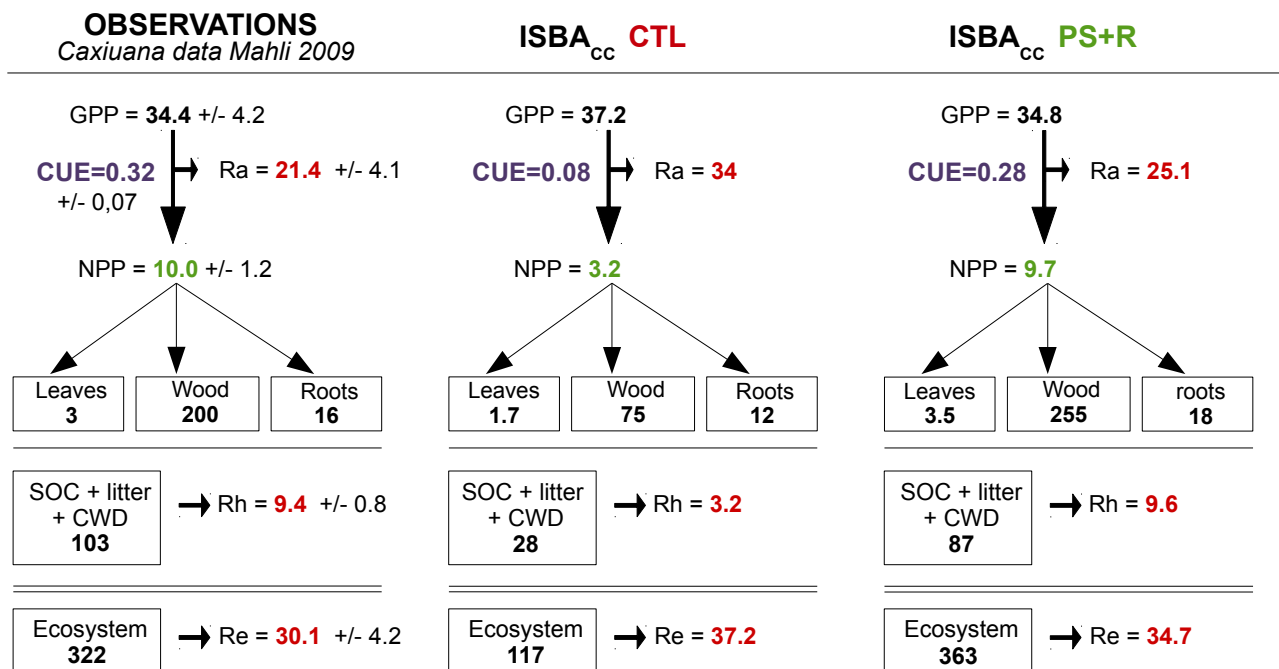


FIGURE 9 – Annual carbon pools (in $tC\ ha^{-1}$) and fluxes (in $tC\ ha^{-1}\ yr^{-1}$) from a synthesis of observations at Caxiuana (Mahli et al. 2009) compared to ISBA_{CC} (CTL and PS+R simulations). Adapted from Randerson et al. (2009).

TABLE 5 – Mean annual autotrophic and heterotrophic carbon stocks and respiration flux deduced from the synthesis of observations done by Malhi et al. (2009) and simulated by *ISBA_{CC}* (simulations CTL and PS+R) at Caxiuanã, K67 and M34. Stocks are in $tC\ ha^{-1}$ and fluxes in $tC\ ha^{-1}\ yr^{-1}$. The ratio defines the % of carbon respired per carbon pool.

		Caxiuanã			Santarem K67			Manaus M34		
		Auto	Hetero	EcoS	Auto	Hetero	EcoS	Auto	Hetero	EcoS
Stocks	OBS	218.7	103.3	322	166.7	171.5	338.2	199.9	141.0	340.9
	PS+R	276.6	87.1	363.7	250.6	98.5	349.2	276.3	150.1	426.4
	CTL	89	27.7	116.7	74.3	29.9	104.2	93.5	51.6	145.1
Resp	OBS	21.4 ± 4.1	9.4 ± 0.8	30.1 ± 4.2	14.9 ± 4.2	14.9 ± 1.4	29.8 ± 4.4	19.8 ± 4.6	9.6 ± 1.2	29.3 ± 4.7
	PS+R	25.2	9.6	34.8	22.5	8.6	31.1	25.0	9.6	34.7
	CTL	33.9	3.2	37.2	30.3	2.8	33.1	32.2	3.5	35.7
Ratio %	OBS	9.8	9.1	9.4	8.9	8.7	8.8	9.9	6.8	8.6
	PS+R	9.1	11.0	9.6	9.0	8.7	8.9	9.0	6.4	8.1
	CTL	38.1	11.6	31.9	40.8	9.4	29.8	34.4	6.8	23.9